



Progress towards a phenomenological picture and theoretical understanding of glassy dynamics and vitrification near interfaces and under nanoconfinement ^{EP}

Cite as: J. Chem. Phys. **151**, 240901 (2019); <https://doi.org/10.1063/1.5129405>

Submitted: 27 September 2019 • Accepted: 07 November 2019 • Published Online: 30 December 2019

 Kenneth S. Schweizer and  David S. Simmons

COLLECTIONS

 This paper was selected as an Editor's Pick



View Online



Export Citation



CrossMark

ARTICLES YOU MAY BE INTERESTED IN

[Polymer physics across scales: Modeling the multiscale behavior of functional soft materials and biological systems](#)

The Journal of Chemical Physics **151**, 230902 (2019); <https://doi.org/10.1063/1.5126852>

[Configurational entropy of glass-forming liquids](#)

The Journal of Chemical Physics **150**, 160902 (2019); <https://doi.org/10.1063/1.5091961>

[Inertial effects of self-propelled particles: From active Brownian to active Langevin motion](#)

The Journal of Chemical Physics **152**, 040901 (2020); <https://doi.org/10.1063/1.5134455>

Lock-in Amplifiers
up to 600 MHz



Zurich
Instruments



Progress towards a phenomenological picture and theoretical understanding of glassy dynamics and vitrification near interfaces and under nanoconfinement

Cite as: J. Chem. Phys. 151, 240901 (2019); doi: 10.1063/1.5129405

Submitted: 27 September 2019 • Accepted: 7 November 2019 •

Published Online: 30 December 2019



View Online



Export Citation



CrossMark

Kenneth S. Schweizer^{1,a)}  and David S. Simmons^{2,b)} 

AFFILIATIONS

¹Departments of Materials Science, Chemistry and Chemical & Biomolecular Engineering, Materials Research Laboratory, University of Illinois, Urbana, Illinois 61801, USA

²Department of Chemical and Biomedical Engineering, University of South Florida, Tampa, Florida 33620, USA

^{a)}kschweiz@illinois.edu

^{b)}dssimmons@usf.edu

ABSTRACT

The nature of alterations to dynamics and vitrification in the nanoscale vicinity of interfaces—commonly referred to as “nanoconfinement” effects on the glass transition—has been an open question for a quarter century. We first analyze experimental and simulation results over the last decade to construct an overall phenomenological picture. Key features include the following: after a metrology- and chemistry-dependent onset, near-interface relaxation times obey a fractional power law decoupling relation with bulk relaxation; relaxation times vary in a double-exponential manner with distance from the interface, with an intrinsic dynamical length scale appearing to saturate at low temperatures; the activation barrier and vitrification temperature T_g approach bulk behavior in a spatially exponential manner; and all these behaviors depend quantitatively on the nature of the interface. We demonstrate that the thickness dependence of film-averaged T_g for individual systems provides a poor basis for discrimination between different theories, and thus we assess their merits based on the above dynamical gradient properties. Entropy-based theories appear to exhibit significant inconsistencies with the phenomenology. Diverse free-volume-motivated theories vary in their agreement with observations, with approaches invoking cooperative motion exhibiting the most promise. The elastically cooperative nonlinear Langevin equation theory appears to capture the largest portion of the phenomenology, although important aspects remain to be addressed. A full theoretical understanding requires improved confrontation with simulations and experiments that probe spatially heterogeneous dynamics within the accessible 1-ps to 1-year time window, minimal use of adjustable parameters, and recognition of the rich quantitative dependence on chemistry and interface.

Published under license by AIP Publishing. <https://doi.org/10.1063/1.5129405>

I. INTRODUCTION

Diverse glass-forming liquids exhibit profound alterations of their dynamics in the nanoscale vicinity of interfaces. These changes can involve shifts in the local or film-averaged glass transition temperature of 50 K or more (increase or decrease), inferred shifts of relaxation time of eight decades or more, and large changes in other dynamic and mechanical properties such as viscosity, elastic

modulus, and diffusion constant.^{1–9} They occur in experimental systems as diverse as block copolymers,^{10–17} layered polymers,^{14,18–21} ionomers,^{22–26} semicrystalline polymers,^{27–34} polymer nanocomposites,^{35–42} polymeric nanoparticles,^{43–45} filled elastomers,^{46–49} supercooled liquids in nanopores,^{50,51} and micellar droplets,⁵ in addition to the baseline class of systems discussed here—thin films of atoms, colloids, molecules, and homopolymers [see Fig. 1, rendered with Visual Molecular Dynamics (VMD)⁵²]. These effects have

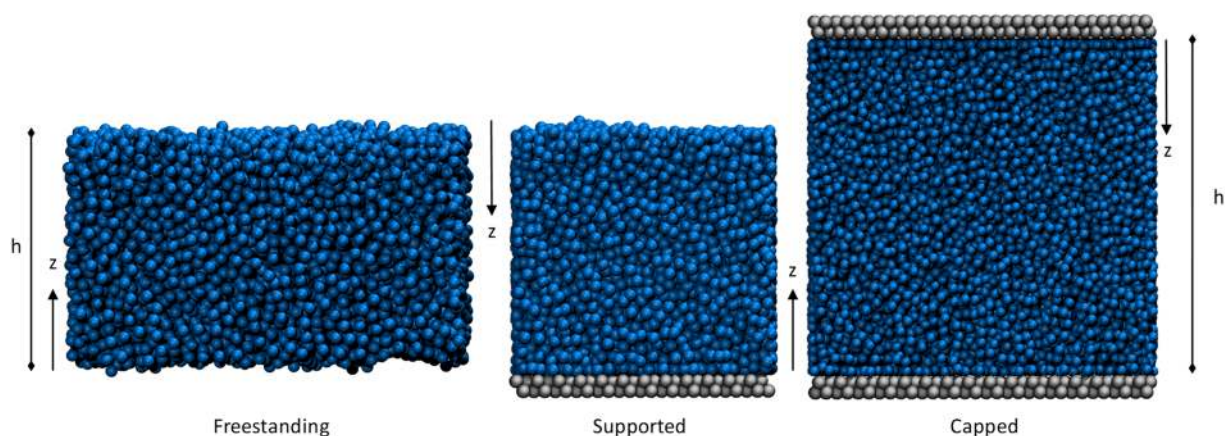


FIG. 1. Visualizations of simulations of freestanding, supported, and capped films, with the latter two employing crystalline walls as substrates. Blue beads are polymer repeat units; gray beads are crystalline walls. In general, one defines a film thickness h and a distance from the interface z . The latter can be defined relative to either interface, with the two z 's being physically nonsymmetric in the supported film only. For all interfaces, the precise microscopic dividing surface ($z = 0$) is a matter of convention. Simulations employ periodic boundary conditions in the directions parallel to the interfaces (normal to z).

significant implications for the design and performance of nano-structured materials with applications ranging from micro-electronics fabrication⁵³ to structural materials to next-generation energy generation and storage devices.^{54,55} Alterations in mobility at free surfaces are also critical to the creation of vapor-deposited ultra-stable glasses^{56–58} and to translational diffusion at vapor surfaces, which can be 4–10 decades faster than expected in a bulk material at the glass transition temperature T_g .^{59,60} From a fundamental standpoint, the field has been partially motivated by the proposition that studying confined glass-forming liquids may elucidate underlying key length scales and mechanisms of the glass transition in the homogeneous and isotropic bulk state.^{2,61–64}

The origin of large near-interface alterations in dynamics and glass formation behavior has been a major open question over the past 25 years.^{1,3–6,62,65,66} The most fundamental issue is the nature of near-interface *spatial gradients* in dynamical and mechanical properties. Although experiments can probe the deeply super-cooled low temperature regime, they typically cannot directly measure these spatial gradients at the nanometer scale. Instead, they commonly only infer limited coarse-grained information from film-averaged measurements, often via a binary 2-layer description. Simulations can probe dynamical gradients with high spatial resolution, but they typically access only 3–6 decades of the relaxation time in coarse-grained models over a temperature range far above the laboratory T_g .

Nevertheless, much progress has been made using simulations, which have evolved⁶⁷ from accessing temperature ranges corresponding to only 2–3 decades of bulk relaxation time variation 15–20 years ago^{68–72} to temperatures accessing 5–6 decades in the longest simulations today,^{67,73,74} with a much larger body of important simulation work in the vicinity of 4 decades. Simulations indicate that the gross phenomenologies in diverse systems with analogous interfaces are quite similar.⁷⁵ Alterations in dynamics appear to be dominated by interfacial effects rather than a finite-size length-scale truncation effect, with these effects ‘nucleated’ at the interface and transferred into the material to

create a mobility gradient.² Sample-averaged measures of T_g shifts and dynamics reflect some weighted average over this gradient, with the direction of change depending on chemical details of the interface including “softness,” topographical roughness, and attractive interactions with the liquid film. Based on simulations, the form and range of dynamical gradients appear to be qualitatively similar across diverse systems, suggesting a possible common underlying leading order mechanism.⁷⁵ However, chemical details do play a quantitatively large role in determining the absolute magnitude and direction of effects.

Intuition suggests that interfacial dynamics are somehow related to their *bulk* glassy analog, although this connection is complicated by the presence of anisotropy and symmetry-breaking near interfaces. Despite the many proposed theoretical frameworks for the bulk glass transition, there is a lack of broad consensus regarding its mechanistic origin.^{63,76,77} This is due, in part, to a paucity of successful efforts to systematically confront theories with empirical data without the introduction of adjustable parameters, which limits their discrimination and falsification. A similar situation exists for the putatively more difficult problem of spatially heterogeneous interface-induced effects on glassy dynamics and T_g . Many theoretical ideas have been proposed, but meaningful progress requires a systematic effort to empirically falsify or validate the various propositions. Here, we focus on progress and key next steps toward answering this question: *to what extent does any proposed theory of glass formation and dynamics near interfaces and under nanoconfinement predict and explain the empirical phenomenology?* We discuss this within the context of four guiding principles:

- (1) By the term “glass transition,” we refer to the practical dynamic arrest process, wherein relaxation times grow dramatically on cooling and ultimately exceed the experimental or simulation time scale. We believe that the ultimate theoretical goal should be to predict *dynamics*, and any causal connection with equilibrium structural or thermodynamic properties, near interfaces.

- (2) Efforts to distinguish between distinct theories should focus on testable predictions within the 1 ps to 1 year range that defines the dynamical window that is empirically accessible via the combination of experiment and simulation.
- (3) Theories should strive to confront empirical data without introducing adjustable fit parameters, given lessons learned from the bulk glassy dynamics problem regarding the inability to distinguish between distinct physical ideas if multi-parameter fit functions are invoked. Ideally, this would be done with the use of *no* adjustable parameters, but perhaps a more realistic intermediate goal is for theory to test concrete predictions against simulation or experiment for multiple physical properties with *minimal* adjustable parameters.
- (4) Given the strong role of chemical details of the interface and liquid in determining the magnitude and direction of interfacial effects on dynamics, prediction of chemistry dependence should be a key theoretical goal, both for its importance to materials science and because these dependences potentially point to and constrain the underlying physical mechanisms.

With these principles in mind, we begin by describing major phenomenological aspects of near-interface glassy dynamics that have emerged from experiments and simulations and that provide promising targets for empirical confrontation with theory. We then survey the extent to which various theoretical frameworks accord with this phenomenology and discuss, where available, theoretical predictions that can potentially be tested in future experiments and/or simulations. Finally, we identify emerging opportunities to better confront theory with empirical data. Throughout this article, we focus primarily on perhaps the simplest and most widely studied class of systems: thick and thin films with one or two interfaces of diverse nature.

II. PHENOMENOLOGY

Progress toward an understanding of interface effects on glassy dynamics has been hindered by experimental complexities and limitations. The real-world phenomena depend on many factors, including the softness and structure of the confining interface, strength of interfacial attractive interactions, temperature relative to the bulk T_g , chemistry, and the nature and time scale of measurement method. Recent work has found that interpretation of the most commonly measured film-averaged experimental probes of dynamics and glass formation is complicated by several confounding factors:

- Sample averaged measures of T_g and other observables can reflect nonlinear weightings over dynamical gradients that can be strong, nonintuitive, and technique dependent.^{8,78–90}
- The strength of observed interfacial effects can depend appreciably on temperature, chemistry, and the time scale or frequency of measurement.^{61,91–95}
- “Two-layer” models (a near interface layer plus bulk layer description) have historically been employed to interpret a substantial fraction of sample-averaged data but do not faithfully reflect the microscopic reality of near-interface dynamics and continuous gradients.

For these and other reasons, while experimental data have played a central role in revealing the presence of alterations in dynamics near interfaces and elucidating the contours of its macroscopic effects, it is extremely challenging to extract from experiments alone a general microscopic picture of glassy dynamics near interfaces.

Simulations have provided some of the most direct data regarding spatially resolved dynamical changes near interfaces, and over the last decade, they have led to a rich picture of the microscopic phenomenology. The fairly small time scales accessible to molecular dynamics simulations do raise questions regarding whether they reflect the physical behavior probed in experiments. Several factors appear to at least partially mitigate this challenge. First, recent simulations report on longer relaxation times approaching 100 ns–1 μ s.^{63,67,73} This often exceeds the experimental dynamic crossover time scale to the deeply supercooled regime of bulk glass-formation physics,^{77,85,96–100} and it also approaches the upper range of frequencies accessible to typical thin film experiments (in most cases, at most 10^5 – 10^6 Hz via dielectric spectroscopy¹⁰¹). Second, recent long-time simulations have observed an apparent saturation (or near-saturation) of the intrinsic length scale of dynamical gradients of relaxation, suggesting that, at least in thin films, simulations can reach the effectively low-temperature limit for this aspect of the problem.^{73,74,102} Third, the simulation-based scenario accords with experiments at much longer time scales in multiple respects. For example, simulations often find that the film-averaged glass transition temperature as a function of film thickness, $T_g(h)$, when *normalized* to the computed bulk T_g , is very similar, in both magnitude and functional form, as to what is observed experimentally, despite the 7–10 decades of relaxation time difference.^{2,9,103} The physical reason for this correspondence has remained poorly understood and is discussed below.

With the above in mind, we now discuss specific aspects of the phenomenology of near-interface dynamics and glass-formation that in our view provide key points of comparison with theory. Our initial focus is on dynamics near vapor surfaces since its phenomenology appears to involve the highest degree of universality. General aspects of solid surface systems are also discussed, followed by the dependence on nonuniversal details of the confining interface.

A. Interfacial origin

Extensive evidence from simulation and experiment indicates that alterations in film-averaged dynamics and T_g are primarily driven by an interface effect rather than by a finite size truncation of a bulk length scale. Early direct evidence for this was provided by fluorescence measurements (which effectively probe local density) of gradients in T_g at the surface and substrate of a supported polymer film.¹⁰⁴ Subsequent studies with this pseudothermodynamic method measured T_g gradients near various polymer interfaces, with a return to bulk-like behavior observed at a sufficient distance from the interface.^{20,21,105} However, the minimum resolvable feature of the gradient was greater than 10 nm such that each reporting layer averaged over a substantial fraction of the gradient. Recent extension of this method to microphase-separated block copolymers has yielded the first reports of dynamical gradients

approaching a nanometer resolution.¹⁷ While these methods suggest significant *quantitative* nonuniversality associated with the material and constraining interface, the results appear consistent with qualitative universality of dominance by surface-induced dynamical gradient effects.

Direct dynamical measurements also yield results consistent with an interfacial origin of these effects. They typically extract information about the dynamical gradient based on an operational two-layer description, wherein a film has a perturbed region close to the interface and a bulk-like region farther away. Experimental probes of time-dependent dye reorientation by Paeng and Ediger,^{106–108} while not spatially resolved, have indicated the presence of a fast process *below* the bulk T_g in freestanding polymer thin films that can be most rationally attributed to a liquid-like surface “mobile layer” that exhibits faster relaxation than the criterion for bulk vitrification (~ 100 s). For example, in polystyrene (PS) thin films, the fast process relaxation time at a temperature only 5 K below the bulk T_g is 10 000 times smaller than expected from bulk behavior. The average relaxation time of this process exhibits a much weaker temperature dependence (roughly Arrhenius) than the bulk liquid. Its associated time correlation function appears to be more nonexponential (stretched) than in the bulk,¹⁰⁸ suggesting the existence of a broad dynamical gradient near the vapor surface. The inferred thickness of this gradient varies from approximately 4 to 8 nm (depending on polymer chemistry) near the bulk T_g , shrinks with cooling, and vanishes at $\sim(0.88$ to $0.92) T_{g,bulk}$, when its relaxation time exceeds the experimental time scale.

An alternative probe of a surface liquid layer is to measure how nanoparticles embed into the vapor surface of glassy polymer films.^{92,109,110} Results are consistent with a liquidlike layer of significant thickness, which shrinks with cooling.^{8,82} These measurements are potentially not of a linear response nature and involve mechanics issues that may complicate their interpretation.¹¹¹ However, viscoelastic measurements point toward a similar physical picture. Measurements of surface recovery after nanoindentation suggest the presence of a mobile layer that persists to low temperatures.⁹¹ Observations of viscous capillary leveling of a step change in the thickness of a polymer film near T_g reveal a transition from whole-film bulk flow to surface-only flow near T_g , indicative of a surface mobile region.¹¹² The most direct spatially resolved evidence from viscous measurements, using a noncontact shear rheometry method, found a viscosity reduction at the surface of a low-molecular-weight glass-forming polymer film with a corresponding viscosity enhancement at the substrate.¹¹³

Simulations also strongly suggest a dominant role for interfacial gradients in systems as diverse as freestanding films,^{68,73,81,82,103,114–122} supported films,^{68,122–125} capped films,^{2,69–72} polymer nanocomposites,^{35–37} polymeric nanoparticle liquids,⁴⁵ ionomers,^{25,26} nanolayered polymers,¹⁹ self-assembling block copolymers,^{16,126,127} and semicrystalline polymers.³⁴

There is perhaps some limited experimental evidence for genuine finite size confinement effects on the glass transition of certain liquids in small pores¹²⁸ and perhaps other systems such as droplets or micelles,⁵ but its generality remains unclear. The extensive evidence surveyed above indicates that such effects do not play the dominant role in a large fraction of confined glass-forming liquids.

B. Onset phenomena and nature of dynamical relaxation gradients

The spatial form, amplitude, range, temperature and density dependences, and low-temperature fate of the dynamical gradient provide some of the most fundamental and potentially useful data to distinguish between different proposed theories. A combination of simulation and experiment points to the following phenomenological picture:

- Interfacial dynamical gradients smoothly evolve as a function of control parameters but only become pronounced for relaxation times above a nonuniversal “onset” time scale τ^* (i.e., below an onset temperature T^*). The chemistry and relaxation function dependences of this onset remain poorly understood, but the results of distinct experimental and simulation studies suggest that it may depend considerably on nonuniversal factors.
- Beyond the onset condition, whole film and local relaxation times obey a power law decoupling relationship with the bulk relaxation time.⁸⁹ This implies that the effective activation barrier in a thin film (or near a single interface) is composed of two contributions that enter in a multiplicative manner: one reflecting a position-invariant but temperature-dependent bulk behavior and a second temperature-insensitive (at low temperatures) but position (distance from an interface)-dependent modification of the barrier.
- Many simulations^{2,68,69,71,72,74,102,129} suggest that the relaxation time gradient is of a double-exponential functional form, implying that the underlying barrier recovers its bulk value exponentially with increasing distance from the interface.⁷³
- The *intrinsic* dynamical gradient spatial range saturates or nearly saturates upon cooling at time scales accessible to simulation, and this saturation is *not* generally associated with a return to bulk Arrhenius relaxation.

1. Temperature-dependence: Onset and decoupling

We first consider two interrelated features of the dynamical gradient that define its temperature dependence: its onset criterion and the factorization of its thermal and spatial dependences.

Experiment and simulation point to a distinct *nonuniversal* onset condition of strong interfacial effects on glassy dynamics. Such an onset phenomenology was originally deduced in experiments via the “fan plots” of Fakhraai and co-workers^{61,92–94} based mostly on cooling-rate-dependent measurements of the ellipsometric T_g for films of various thicknesses. A smaller set of experiments probed surface viscous relaxation⁹¹ or film dewetting.⁹⁴ Because these measurements cannot probe dynamics in films significantly above the bulk T_g , they typically employ an empirical Arrhenius extrapolation from inferred relaxation times near or slightly below the “conventional” 100 s bulk T_g . Based on an approximate intersection of these extrapolations from multiple thickness films or from surface and bulk dynamics, it was inferred for several systems that a return to bulk or near-bulk dynamics occurs at temperatures modestly above T_g and at time scales modestly less than the timescale of T_g (see Fig. 2, top). This defines an apparent onset of strong interfacial alterations in dynamics upon cooling. Such behavior is also likely

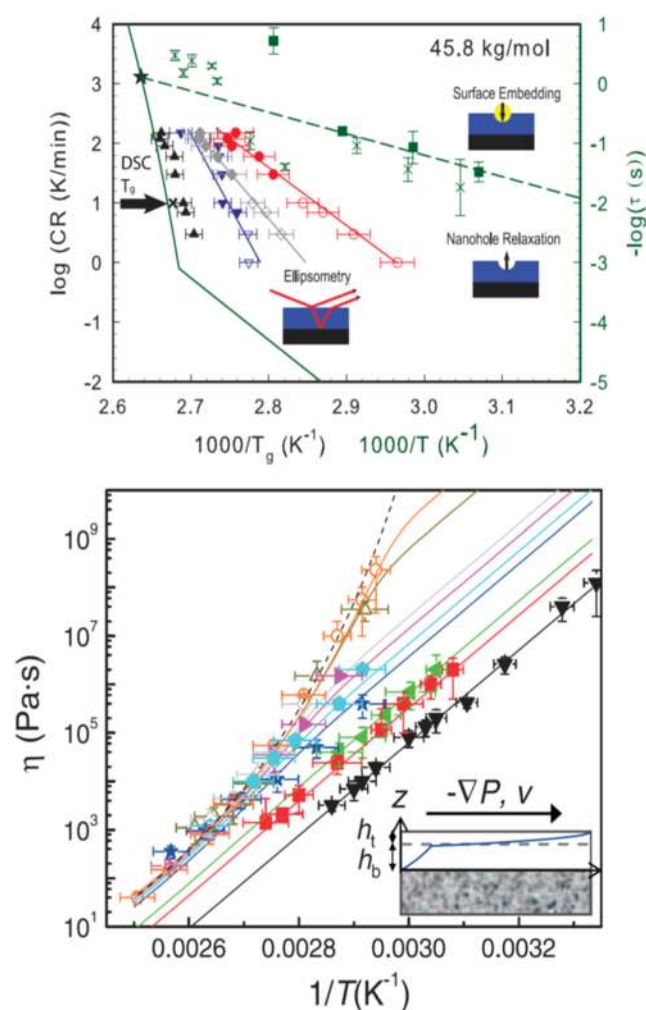


FIG. 2. (Top) Plot of logarithmic cooling rate vs inverse glass transition temperature as determined via ellipsometry for films of thickness 8 nm (red circles), 18 nm (gray triangles), 45 nm (blue inverted triangles), and 274 nm (black triangles); relaxation time vs inverse temperature for surface nanoparticle embedding (green 'x's) and surface nanohole relaxation (green squares). Reproduced with permission from E. C. Glor and Z. Fakhraei, *J. Chem. Phys.* **141**, 194505 (2014). Copyright 2014 AIP Publishing LLC. (Bottom) Logarithmic plot of film viscosities vs inverse temperature for films of multiple thicknesses obtained via film breakup experiments. From bottom to top, data sets correspond to films of thickness 2.3, 4, 5, 9, 11, 14, 17, 50, and 79 nm. Reproduced with permission from Yang *et al.*, *Science* **328**, 1676 (2010). Copyright 2010 American Association of the Advancement of Science.

reflected⁹³ in the observation that dynamical measurements in thin films performed at high enough frequency and temperature often exhibit little perturbation from bulk dynamics.^{130–132}

A different, explicitly dynamical, approach by Tsui and co-workers (Fig. 2, bottom) probed the temperature-dependent film-averaged viscosity of low-molecular weight polystyrene (PS) down to extremely thin films.¹³³ Their results also exhibit an onset temperature, but its quantitative value and time scale are very different from the findings described above.^{61,92–94} A direct comparison

with the results of Fakhraei and co-workers is possible, as PS was studied by both groups. Whereas the cooling-rate-dependent ellipsometry measurements reported that strong interfacial effects begin only a few kelvin above the bulk T_g, the rheological measurements found the onset to be ~40 K above the bulk T_g. This translates to a massive difference in onset *time scales*: the cooling-rate-ellipsometry-T_g work implies an onset within several decades of the conventional bulk vitrification time scale, whereas the viscosity measurements imply an onset at ~7 to 8 decades of shorter time scales. It is unlikely that this difference results from any dependence on polymer molecular weight, given that the cooling-rate ellipsometry-T_g measurements have also reported a near-T_g onset in small-molecule glass-formers.^{61,92–94} Instead, it seems that the measure of stress relaxation or viscous flow employed by Tsui and co-workers exhibits strong interfacial effects at much higher temperatures (smaller relaxation times) than dilatometric probes of dynamics, implying that the onset time scale is nonuniversal even at fixed chemistry.

Recent simulations of coarse polymer models and vapor interface films likewise identify a time scale at which a high-temperature regime of weak or absent interfacial dynamical effects transitions to strong effects at lower temperatures. The temperature dependence of dynamics in the latter regime is characterized by an intriguing fractional power-law “decoupling relation” (Fig. 3),⁷³

$$\frac{\tau(T, z)}{\tau_{\text{bulk}}(T)} = \left(\frac{\tau_{\text{bulk}}(T)}{\tau^*(z)} \right)^{-\epsilon(z)}, \quad (1)$$

where $\tau(T, z)$ is the alpha relaxation time at a temperature T and distance z from the interface, the subscript “bulk” here and elsewhere denotes the value of the given property in the bulk state [here $\tau_{\text{bulk}}(T)$ refers to the bulk alpha relaxation time at a temperature T], ϵ is a temperature-invariant (at sufficiently low temperature) “decoupling exponent,” and $\tau^*(z)$ is an effective onset time scale of this decoupling relation (based on an upward extrapolation from low temperatures) that in practice depends at most weakly on the position in the film. These simulations indicated that τ^* corresponds closely to a crossover at which ϵ transitions from a very small or zero value at high temperatures (weak/no decoupling) to a larger and temperature invariant value in the low temperature limit. When the bulk relaxation time is less than this time scale (which was reported to be in the vicinity of 1–10 ps for segmental translational dynamics in a bead-spring polymer model), the interfacial effect on the barrier is considerably muted or even absent.⁷³ Beyond this onset time scale, the local dynamics near an interface progressively diverge from the bulk dynamics with increasing cooling per Eq. (1).

The physical significance of Eq. (1) is discussed in detail below; here, we first focus on the onset and nonuniversality aspects. Further elucidation of the connection of the onset effect observed on simulation time scales to its experimental analog is needed. Evidently, the onset time scale observed in coarse-grained polymer simulations is far shorter than for ellipsometric measurements on molecular and polymeric liquids,^{61,92–94} and modestly shorter than that found in the viscosity measurements.¹³³ Given the contrast between onset behavior observed via different experimental methods discussed above, this likely reflects an unavoidable dependence on relaxation function

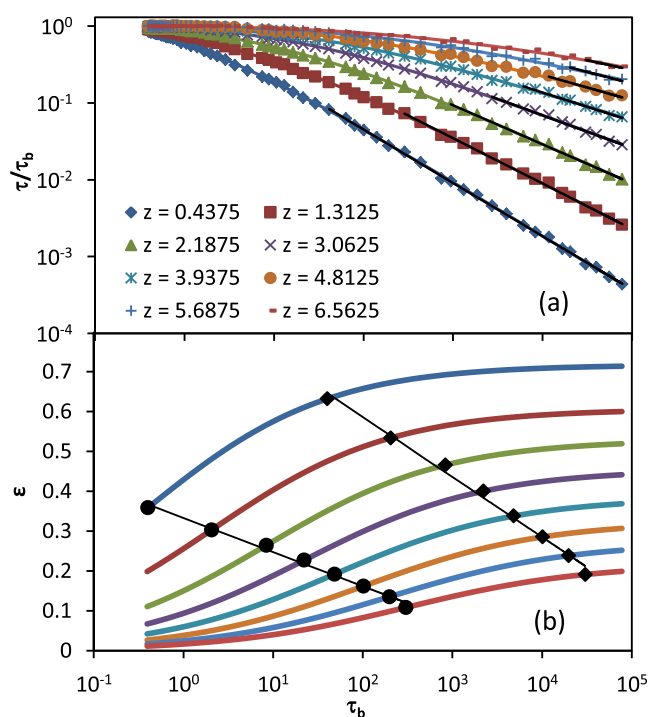


FIG. 3. Plot, vs τ_{bulk} , of (a) τ/τ_{bulk} , where in this figure $\tau_b = \tau_{\text{bulk}}$, illustrating low-temperature limiting fractional power law decoupling behavior for multiple layers within a film at the noted distances from the interface (in units of monomer diameter) and (b) decoupling exponent ϵ for these same layers obtained via a fit and differentiation of data in part (a), illustrating the onset of a well-developed regime of constant ϵ in Eq. (1) at long relaxation times/low temperatures. Reproduced with permission from D. Diaz-Vela, J.-H. Hung, and D. S. Simmons, ACS Macro Lett. 7, 1295 (2018). Copyright 2018 American Chemical Society.

and, potentially, chemistry. Simulations most commonly report on the self-part of the intermediate scattering function at the segmental scale. This quantity probes single particle translational motion and is rarely, if ever, measured in experiments on films in a time-resolved manner. Rather, the potentially relevant neutron scattering methods have signal resolution and sensitivity limitations that have, to date, largely precluded their use to probe this type of dynamical quantity in thin films in a time-resolved manner. One simulation study of reorientational dynamics reported relatively weak¹¹⁴ nanoconfinement effects, which may suggest that the onset time scale may be shifted to longer time scales for these relaxation functions in at least some cases. This effect is reminiscent of “translation-reorientation” decoupling in bulk dynamically heterogeneous supercooled liquids,^{134–136} although this potential connection requires additional investigation. At the same time, the generality of this finding and its dependence on chemistry are unresolved, and these issues should be a high priority for future research given the practical and fundamental importance of variations of the onset time scale.

The finding of a much earlier onset of strong interfacial alterations in translational relaxation of bead-based simulation models

can be intuitively rationalized if the sensitivity of glassy dynamics to interfaces is dominated by an emergent low-temperature barrier reflecting the collective physics in deeply supercooled liquids. In bulk experiments, it is found that T_g often must be sufficiently closely approached before the cooperative component of the effective barrier that underlies non-Arrhenius relaxation becomes dominant.^{137–139} This is likely not the case in coarse grained model simulations, which are characterized by much smoother potential energy landscapes than real chemistries. As a consequence, they have lower high-temperature activation barriers, which results in dominance of cooperative dynamics at relatively higher temperatures. This idea is supported by experimental studies of bulk supercooled molecular and polymer liquids by Rössler *et al.*,^{137–139} which find an Arrhenius regime at high temperatures with barriers significantly larger than those in coarse-grained simulation models. If this scenario is correct, it could resolve the longstanding question of why simulations exhibit dynamical interface effects comparable to experiments despite probing many decades of shorter time scales. It might also provide a basis for understanding the chemistry dependence of interfacial glassy dynamics and nanoconfined T_g as determined based on a fixed time scale or cooling rate: materials and relaxation functions with lower (higher) onset time scales (temperatures) naturally exhibit stronger alterations in near-interface dynamics in a fixed time scale measurement.

Any dependence of the onset condition on relaxation function and chemistry is important theoretically, since most theories do not specify *which* relaxation function they model. Such a simplification may not be as reliable under confinement as it is in the bulk. The above comparison of viscosity and ellipsometric data indicates that the assumption that these processes generally track each other may fail dramatically in thin films.^{133,140} Moreover, these findings highlight an urgent need for new simulation and experimental work probing the relaxation function and chemistry dependence of the onset condition of strong nanoconfinement effects.

Equation (1) also provides a key insight into the nature of near-interface dynamics at temperatures beyond the onset. The most dramatic implication is that the activation barrier near interfaces in the low temperature limit can effectively be *factored* into a purely temperature-dependent part reflecting solely the physics of *bulk* activated dynamics, and a purely position-dependent factor reflecting a rescaling of the bulk barrier near the interface,⁷³

$$\Delta E(T, z) = (1 - \epsilon(z))\Delta E_{\text{bulk}}(T). \quad (2)$$

Notably, only the assertion that dynamics are activated is required to infer Eq. (2) from Eq. (1), provided that ϵ is temperature-invariant over the temperature range under consideration. Equation (2) suggests a massive underlying simplicity of the temperature dependence of the relaxation time in films and near interfaces: multiplicative reduction of the effective barrier. While it is difficult to directly test Eqs. (1) and (2) experimentally over a wide range of temperatures, such behavior is plausibly consistent with the work of Fakhraai *et al.*,^{61,92–94} who generally find that experimental data at low temperatures can be empirically treated as reflecting a thickness-dependent reduction of the effective activation barrier. Because the experimental data span a very limited range of low temperatures, they alone cannot establish that Eq. (2) holds. However, the observation of Eq. (1) in the simulation, combined with an apparent

Arrhenius relaxation process over a narrow range of temperatures, would lead to the observed qualitative experimental behavior.

The above phenomenology has potential implications for why the ratio of the average glass transition temperature in a film of thickness h to its bulk analog, $T_g(h)/T_{g,bulk}$, deduced from simulation and experiment is often very similar despite the enormous difference in time scales involved. One of us has shown that Eq. (1) combined with a Vogel-Fulcher-Tammann (VFT) empirical description of the temperature dependence of dynamics near T_g ^{141–143} leads to⁷³

$$\frac{T_g(h) - T_{0,bulk}}{T_{g,bulk} - T_{0,bulk}} = (1 - \varepsilon(h)) \left(1 - \frac{\ln \tau_0 / \tau_{0,bulk}}{\ln \tau_g / \tau_{0,bulk}} \right)^{-1}, \quad (3)$$

where $T_{0,bulk}$ is an extrapolated divergence temperature for the bulk state, τ_0 is an extrapolated high-temperature relaxation time for the film within the VFT description (which in general can depend on h), $\tau_{0,bulk}$ is an extrapolated high-temperature relaxation time for the bulk state within the VFT description, and τ_g is a relaxation time chosen by convention as the time scale associated with glass formation (or more generally is the time scale of any fixed-window measurement). One can recast this result in terms of the onset temperature of the strong low-temperature decoupling regime and the mean-film low-temperature decoupling exponent as

$$\frac{T_g(h)}{T_{g,bulk}} = 1 - \varepsilon(h) \left(\frac{1 - f_c(h)}{1 - \varepsilon(h)f_c(h)} \right) \left(1 - \frac{T_{0,bulk}}{T_{g,bulk}} \right), \quad (4)$$

where

$$f_c = \frac{\log \tau^*(h) - \log \tau_{0,bulk}}{\log \tau_g - \log \tau_{0,bulk}} \quad (5)$$

is the fractional distance between the bulk τ_0 and the time scale that defines T_g at which the onset τ^* of strong decoupling is located, and where the dependences on h can generally also be replaced by dependences on z if the equations are applied locally. For measurements well past the onset time, the factor involving f_c goes to 1 such that the local T_g perturbation is directly controlled by the local barrier reduction, $1 - T_g(h)/T_{g,bulk} = \varepsilon(h)(1 - T_{0,bulk}/T_{g,bulk})$.

Equation (4) suggests a potential rationalization of the comparability of *normalized* T_g alterations in the simulation and in experimental measurements of T_g . Specifically, it indicates that T_g changes are controlled by the fractional reduction of the bulk barrier by the factor of $1 - \varepsilon$ and the measurement time scale (τ_g) relative to the onset time scale, τ^* . Taken together, simulation, rheological, and cooling-rate measurements indicate that the onset time scale can depend on chemistry and relaxation function. If the onset time scale for translational dynamics in flexible bead-based polymer simulation models is indeed ~ 1 to 10 ps, then the longest time scales computationally probed are approximately the same distance past their onset as the cooling-rate ellipsometric measurements are past their onset. According to Eq. (4), this will lead to comparable effects as measured by T_g on their respective time scales.

As noted above, more work is needed to connect the onset observed in the simulation to that observed in experiments. Efforts to understand the onset and decoupling behavior, at least quali-

tatively, should be a theoretical priority. New simulations are also needed for thick films with a solid substrate to test the generality and universality of the decoupling phenomenon.

2. Spatial variation

How does the relaxation time near an interface vary in space for temperatures below the onset? Many simulation studies over the past 15 years for *both* solid and vapor surfaces have examined the form of the relaxation time gradient, $\tau(z, T)$. It is widely reported to be empirically well described by a “double-exponential” form,^{2,68,69,71,72,74,102,129}

$$\tau(z, T) = \tau_{bulk}(T) \exp \left[-A(T) \exp \left(-\frac{z}{\xi} \right) \right], \quad (6)$$

where the amplitude, A , can be positive or negative depending on the interface. As illustrated in Fig. 4, this double-exponential variation has been seen in a variety of studies at different temperatures and for substantively different models of the liquid and interface. The majority involve values of ξ in the range of approximately 2–3 bead diameters, with the amplitude A corresponding to a 2–4 decade modification of τ at the surface.

This is an important finding, since the functional form of the interfacial gradient is a key feature for which distinct theories strongly differ. However, questions arise. First, is Eq. (6) purely an empirical fit or does it reflect fundamental physics? Second, does Eq. (6) reflect the low temperature behavior or is it a crossover behavior characteristic of the relatively high temperatures probed in simulations? Third, how can one understand the nonuniversal magnitude and temperature dependence of the amplitude, $A(T)$? Finally, how large is the exponential “intrinsic” dynamical correlation length, ξ , and how does it change with temperature, density, and chemistry?

The very recent vapor interface simulation work by one of us⁷³ employing the above decoupling analysis suggests that Eq. (6) is not simply an empirical fit function. Specifically, the positive $\varepsilon(z)$ in Eq. (1) can be directly extracted from the simulation for any location z by plotting $\log(\tau(z)/\tau_{bulk})$ vs $\log(\tau_{bulk})$. Performing this analysis as a function of z then directly yields $\varepsilon(z)$. Since $1 - \varepsilon(z) = \Delta E(z)/\Delta E_{bulk}$, this corresponds to a direct extraction of the fractional change of the effective barrier as a function of distance from the interface. For films with a vapor interface, where dynamics are locally sped up near the surface, the barrier reduction factors extracted via this method demonstrate that the bulk activation barrier to relaxation is recovered *exponentially* with increasing distance from the interface⁷³ (see Fig. 4, inset), i.e.,

$$\varepsilon(z) = 1 - \frac{\Delta E(T, z)}{\Delta E_{bulk}(T)} = \varepsilon_0 \exp(-z/\xi_{\Delta E}), \quad (7)$$

where $\varepsilon(z)$ is the fractional barrier reduction at a position z , $\Delta E(T, z)$ is the barrier at a temperature T and distance z from an interface, $\Delta E_{bulk}(T)$ is the bulk barrier, and ε_0 is the value of the decoupling exponent at the interface. Combining this with Eq. (1) and a generalized activation model immediately implies an *approximately double-exponential* variation of the relaxation time with z ,

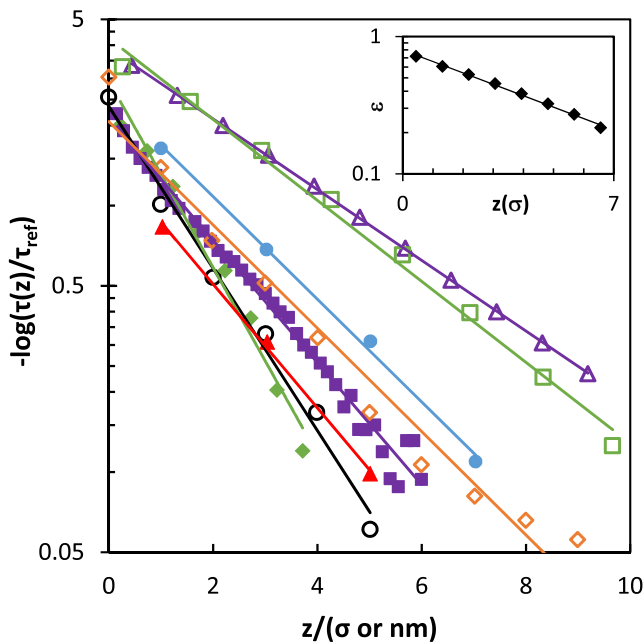


FIG. 4. Double-log plot of τ/τ_{ref} (where τ_{ref} is either the corresponding bulk or midfilm relaxation time) illustrating an empirical double exponential variation of τ with distance from a free surface from a variety of simulation studies: freestanding bead-spring polymer film with $\tau_{bulk} \sim 10^{4.9}$ LJ time units⁷³ (purple open triangles), freestanding bead spring polymer film with $\tau_{bulk} \sim 10^4$ LJ time units¹¹⁹ (green open squares), freestanding bead spring polymer film with $\tau_{bulk} \sim 10^{3.8}$ LJ time units⁶⁸ (blue circles), coarse-grained polystyrene model with $\tau_{bulk} \sim 10^3$ ps¹²¹ (orange open diamonds), coarse-grained poly(methyl-methacrylate) model with $\tau_{bulk} \sim 10^3$ ps¹²¹ (black open circles), interface with smooth confining wall of a binary Lennard-Jones glass former with $\tau_{bulk} \sim 10^3$ LJ time units⁶⁹ (purple squares), free surface of supported bead-spring polymer with $\tau_{bulk} \sim 10^{3.3}$ LJ time units⁶⁸ (red triangles), and united atom polystyrene model with $\tau_{bulk} \sim 10^{2.2}$ ns¹⁰³ (green diamonds). All data sets are digitally extracted from published figures except for that from Vela *et al.*, which is taken from the raw original data. Data are truncated at 0.05 due to large relative uncertainties associated with digital extraction for small values of the ordinate. Several data sets involve shifts on the abscissa where the interface was not at $z = 0$ in the original data set. The points in the inset are limiting low-temperature decoupling exponents ε for a bead-spring polymer as a function of z , with the line illustrating an exponential fit to the data, with a decay length scale of 5.2 bead diameters.⁷³

$$\begin{aligned} \tau(T, z) &= \tau_{bulk}(T) \left(\frac{\tau_{bulk}(T)}{\tau^*(z)} \right)^{-\varepsilon_0 \exp(-z/\xi_{\Delta E})} \\ &= \tau_{bulk}(T) \exp \left[\varepsilon_0 \left(\ln \frac{\tau^*(z)}{\tau_{0,bulk}} - \frac{\Delta E_{bulk}(T)}{kT} \right) \exp(-z/\xi_{\Delta E}) \right]. \quad (8) \end{aligned}$$

If τ^* is constant with respect to z , then Eq. (8) is the double-exponential form and is equivalent to Eq. (6). In that case, the range ξ in Eq. (6) for the $\log(\tau)$ gradient and the range $\xi_{\Delta E}$ in Eq. (8) for the barrier gradient will be equal. We refer to these length scales as the *intrinsic range* of the gradient, which we will contrast below to *practical* gradient ranges describing the distance for recovery of bulk-like relaxation times to within some small difference. In addition, as we

will discuss below, both ξ and $\xi_{\Delta E}$ are observed to be at most weakly temperature dependent.

Thus, both Eq. (6) and the decoupling relation of Eq. (2) can be viewed as a *consequence* of the fundamental barrier factorization property with an exponential spatial variation of the associated exponent. Early work has suggested approximately a two decade shift in the onset time scale τ^* over the exponential decay range of the gradient.⁷³ This is relatively small on the scale of the overall time range relevant to the glass transition, although not negligible. However, at this stage, the generality of this finding is unknown and should not be overemphasized. For weak variation of τ^* with position, the variation of τ with z will still follow the double-exponential form for an appreciable range of z , but with some difference between values of the intrinsic dynamical lengths ξ and $\xi_{\Delta E}$ obtained via Eq. (6) vs Eq. (7). The observation of both exponential barrier gradients and double-exponential τ gradients thus also indirectly suggests that τ^* should be at most weakly dependent on z . We return to the issue of the intrinsic range below.

We note that the relaxation time gradient also directly determines the spatial gradient of the glass transition temperature, $T_g(z)$, based on an adopted vitrification criterion. Hence, the mathematical form of $T_g(z)$ is intimately related to the fundamental relaxation time gradient behavior in Eqs. (1) and (2), the spatial variation of the effective barrier, and the temperature dependence of the bulk relaxation time. For example, an exponential vs double exponential relaxation time gradient is expected to yield *qualitatively* different forms of $T_g(z)$ —approximately linear vs exponential, respectively. Unfortunately, experimentally measuring $T_g(z)$ to high accuracy with nanometer-scale resolution is extremely challenging. Simulations have studied this question based on a relatively short time vitrification criterion. Studies of various polymer models appear to find a roughly *exponential* recovery of bulk-like T_g with increasing distance from the interface, as shown in Fig. 5.¹²⁰ For these results, the fractional suppression of T_g near the surface is $\sim 12\%$ to 25% . For polystyrene, this would correspond to a near-surface reduction of T_g by ~ 44 to 93 K. Notably, these simulation-based estimates are consistent with experimental findings despite the fact that the simulation defines vitrification based on a much shorter absolute time scale than does experiments. The exponential decay range is ~ 2 to 3 elementary bead diameters or nanometers. This would suggest a recovery to within 10% of bulk-like T_g over a range of ~ 10 nm, again consistent with the preponderance of experimental findings. The one exception to this latter range is a simulated united atom model of polystyrene,¹⁰³ where the range is of order 1 nm. However, the discussion above anticipates that the onset time scale of strong nanoconfinement effects is likely appreciably higher for this type of chemically realistic model due to its larger high-temperature “Arrhenius-regime” activation barrier. The shorter range in this system may thus be a signature of not having fully surpassed the onset time scale for this system.

This empirical finding of an exponential spatial variation of T_g is consistent with the exponential recovery of the bulk barrier reported above. Specifically, combining Eq. (4), written at a local level for the time scale and ε dependence of $T_g(z)$ within a VFT model, with the exponential barrier recover [Eq. (7)] similarly yields an exponential near-surface T_g variation when the measurement time scale is well past the onset time scale.

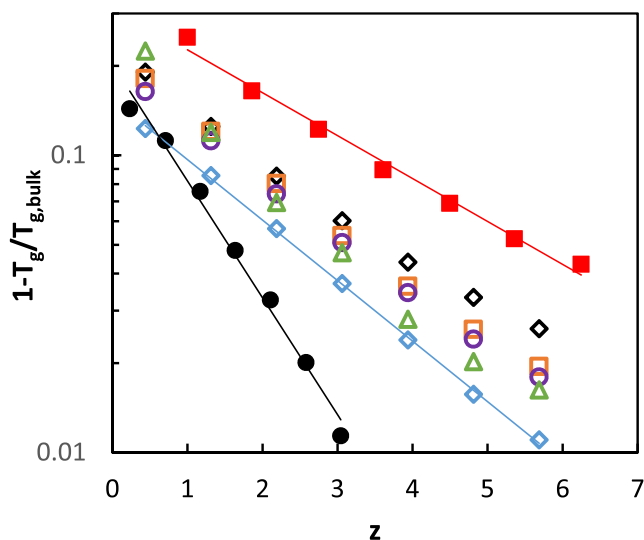


FIG. 5. Fractional dimensionless change in T_g as a function of z as reported from simulations of multiple systems, illustrating the general finding of exponential T_g gradients: the free surface of a supported bead-spring polymer film based upon an extrapolation to 100 s¹²³ (red squares), of a united-atom polystyrene freestanding film¹⁰³ and from simulations of freestanding films of a standard bead-spring polymer (black open diamonds), bead-spring polymer with reduced bond length (orange open squares), bead-spring polymer with monomeric antiplasticizer additives (open blue diamonds), bead-spring polymer with flexible oligomer additives (purple open circles), and bead-spring polymer with stiff oligomer additives (green open diamonds).¹²⁰ Units of abscissa are LJ bead diameters for bead-based models and nanometers for chemically realistic models. Lines are example of best fits to an exponential decay model.

We also note that experimental T_g -gradient data reported by Baglay and Roth for bilayer films indicate that for polystyrene near a softer (dynamically faster) poly(*n*-butyl methacrylate) interface, the bulk T_g is recovered in a roughly exponential manner with increasing distance from the interface,²⁰ consistent with Eq. (4) and an exponential variation of the barrier. However, an open puzzle is that the range of that particular gradient is much larger than that found in nearly all other experimental and simulation studies. The bilayer experiments involve very high molecular weight polymers, and broad (5–7 nm) polymer-polymer interfaces, and the authors suggested that the very long range T_g gradient may be a polymer-specific effect. Christie *et al.* reported T_g gradients in microphase-separated block copolymers with higher spatial resolution and with a range more commensurate with simulations.¹⁷ At present, the number of data points is small and likely in the “ultrathin” film limit (discussed below) where gradients from opposing interfaces interact and obscure the single interface gradient shape. However, this approach is promising for experimental determination of T_g gradients at nanometer-scale resolution.

3. Intrinsic correlation length and limiting low-temperature behavior

We now turn to the critical issue of the *intrinsic* dynamical length scale in Eqs. (6)–(8) and its dependence on temperature. Multiple recent simulations report evidence of a *saturation* or

near-saturation of the intrinsic length scale of the dynamical gradient upon cooling.^{73,74,102} An intrinsic length scale has been determined in two ways: via a direct empirical fit of $\tau(z)$ data to Eq. (6),^{74,102} or by first determining the spatial variation of the barrier via the decoupling analysis [Eqs. (1) and (2)] and then determining the exponential decay constant for recovery of bulk-like barriers via a fit to Eq. (7).⁷³ Because of spatial variation in the onset time scale⁷³ τ^* , these two methods do not generally yield quantitatively identical results, with the decoupling analysis expected to produce a modestly longer length. However, the dynamical range obtained from *both* methods exhibits signs of saturation at low temperatures accessible to simulations.

The effects of this saturation of the intrinsic surface range of barrier modifications are shown in Fig. 3(b), which plots the temperature evolution of the barrier truncation factor ϵ for layers at various distances from a polymer film free surface as a function of bulk relaxation time. The plateau in ϵ at low temperatures naturally corresponds to a saturation of the range over which ϵ varies, with an exponential decay range of ~ 5 segmental diameters obtained in the low-temperature limit in this case.⁷³

More broadly, studies reporting a low-temperature saturation of the intrinsic range include not only systems with a vapor interface but also coarse grained polymer models and diverse spherical particle model liquids near both rough pinned particle surfaces and smooth walls.^{74,102,129,144,145} The low-temperature saturation value is nonuniversal (typically ~ 2 to 5 sphere or bead diameters), but qualitatively is always modest in absolute magnitude. From a practical perspective, this indicates that 90% of the bulk barrier is recovered over a range of order 10 nm or molecular layers from the surface. Via Eq. (4), this implies the presence of a ~ 10 nm domain with appreciably perturbed T_g , which seems consistent with the interpretation of most experiments. We note there is a suggestion^{74,102} that the length scale saturation is only “apparent,” and that if lower temperatures could be simulated it would again grow. At present, this is an untestable hypothesis for which no evidence exists, and the observation of a saturation or near-saturation now extends to 100 ns relaxation time scales.

We emphasize that this *intrinsic* dynamical length must be distinguished from consideration of a *practical* dynamical length of τ perturbations *defined based upon a fractional recovery of bulk relaxation times*.^{68,69,71,72,82,123,124} Given Eq. (6), this latter length scale can and generally *does* grow (often strongly) upon cooling, even if the intrinsic ξ becomes temperature invariant. Specifically, the practical length scale $\xi_{\tau\text{bulk}}$ for recovery of bulk-like τ within some factor will scale as $\xi_{\tau\text{bulk}} \sim \xi \ln(A(T))$. This is a consequence of growth of the amplitude factor⁷³ A in Eq. (6) with cooling, which reflects growth in the *relative* change from the bulk relaxation time at the interface. This amplitude growth is nonuniversal but is a natural outcome of Eq. (8) that $A(T) = \epsilon_0 \Delta E_B(T)/kT$, which grows upon cooling. Hence, the *practical* length scale of recovering the bulk relaxation time (of high relevance to the experiment) can be rather large and temperature-dependent even if the *intrinsic* length ξ is temperature insensitive. Clarification of the variation of the intrinsic dynamic length scale for glassy films seems reminiscent of subtle problems encountered in the extraction of a length scale in higher order dynamic susceptibilities in bulk supercooled liquids.⁶³

Overall, these findings suggesting a saturation or near-saturation of the intrinsic length scale of surface dynamics are of

extreme importance to the theoretical understanding of this problem. As we discuss below, many theoretical frameworks appear to be inconsistent with this behavior. The present early evidence for saturation in multiple systems appears to be compelling, and further testing its generality in more systems and on longer time scales should be a high priority for future work.

C. Role of local structural metrics

A central question in the origin of interfacial dynamic gradients is whether they are locally driven by interfacial modifications of local structure and/or density. Multiple distinct lines of evidence indicate that the answer is no.

First, simulations have found that the local relaxation time and density are not well correlated near interfaces. For example, early work demonstrated that dynamics near smooth vs structured amorphous walls are strongly perturbed in opposite *directions*, despite involving nearly identical perpendicular oscillatory density profiles.² This is in accord with the fact that dynamical gradients commonly extend at least 5–10 nm or particle diameters from the interface, whereas gradients in liquid density are much shorter ranged. Moreover, the *practical* spatial range over which dynamics return to bulk near an interface generally grows with cooling in simulations,^{68,69,71,72} whereas surface density gradients typically *shrink* weakly on cooling.^{82,123}

Second, recent machine learning studies of simple simulated models searched for correlations between changes of local structure [quantified via a local implementation of the radial distribution function, $g(r)$] and interfacial dynamics in freestanding films.¹⁴⁶ It was found that the large dynamical changes near interfaces cannot be predicted from changes of local structure.¹⁴⁶ Importantly, this is qualitatively distinct from the corresponding bulk at similar temperatures, where machine learning finds a strong connection between aspects of the local $g(r)$ and relaxation times.¹⁴⁷

Third, many simulations with solid boundaries under so-called “neutral confinement” conditions have been performed where the substrate is identical to the fluid of interest but is pinned. In this “amorphous boundary condition” protocol, the fluid structure remains the same as in the bulk,^{2,64,74,102,144,145} but very large changes of glassy dynamics are still observed, again supporting an intrinsic *dynamical* origin of interface-induced modification of motion and vitrification.

Taken together, the above studies establish that interfacial gradients of equilibrium structural properties are not the primary driver of large and long range gradients in glassy dynamics. This indicates the centrality of spatial transfer into the material of interface-nucleated purely *dynamical* effects.

D. Mean behavior of “thick” films

Although the fundamental feature of thin-film dynamics is the relaxation time gradient, both practical materials properties and experimental studies aimed at elucidating the underlying physics often focus on some *average* behavior of the entire film. The most commonly measured property is $T_g(h)$. How do such variable-thickness film-averaged properties report on the underlying gradients?

As an illustrative exercise germane to this question of what information can be extracted from film-averaged quantities, we

consider a highly simplified model, wherein a mean film property $\langle \Theta \rangle$ reflects an evenly weighted linear arithmetic average over the locally defined property,

$$\langle \Theta \rangle = \langle \Theta(h) \rangle = \frac{1}{h} \int_0^h \Theta(z) dz. \quad (9)$$

This property could be, e.g., T_g or a relaxation time. In most cases, linear arithmetic averaging holds *at best* for raw relaxation functions and to a good approximation for relaxation times, and not for other quantities such as T_g .⁷⁸ The issue of more complex weighting functions is addressed further below; here, we employ the simple case of linear arithmetic averaging. As a pedagogical calculation, we consider three simple 2-parameter gradient forms and we ask whether they can be reconstructed, or even discriminated between, from film-averaged data. Specifically, we consider the following equations for the gradient in the local value $\Theta(z)$ associated with one interface:

$$\frac{\Theta(z)}{\Theta_{bulk}} = \left(1 - A + \frac{Az}{2\xi} \right) H(2\xi - z) + H(z - 2\xi), \quad (10)$$

$$\frac{\Theta(z)}{\Theta_{bulk}} = 1 - A \exp(-z/\xi), \quad (11)$$

$$\frac{\Theta(z)}{\Theta_{bulk}} = 1 - A + AH(z - \xi). \quad (12)$$

Here, H is the Heaviside step function, A sets the gradient amplitude, and ξ sets its range. These three forms correspond to linear, exponential, and stepwise (2-layer model) gradients of the *local value* of $\Theta(z)$, respectively. The *mean film, thickness-dependent* property $\langle \Theta(h) \rangle$ corresponding to a particular functional form for $\Theta(z)$, is then obtained by combining that form with Eq. (9). To avoid complications that can arise when two gradients interact in very thin films (more on this limit below), here, we consider the simple model of a supported film in which one interface (at $z = h$) is dynamically neutral (no gradient) and assume that the gradient from the other interface (located at $z = 0$) as modeled per the equations above is simply truncated at the neutral interface. The latter assumption may be incorrect, and relaxing it introduces extra complexity for ultrathin films. However, it only appreciably impacts films of thickness comparable to or less than the gradient size.

As shown in Fig. 6, all of these functional forms lead to indistinguishable curves for h appreciably greater than 2ξ . This is a consequence of the fact that when the film is appreciably larger than the gradient size ($h \gg \xi$), the mean film $\langle \Theta(h) \rangle$ is only sensitive to the total, integrated deviation of $\Theta(z)$ from its bulk value over the entire interfacial regime. Specifically, if one defines a region of thickness $a\xi$ (where a is some constant of order one) that contains all of the near-interface material in which Θ is appreciably perturbed from its bulk value, then the average in Eq. (9) can be split into two terms, one involving the interfacial region and the other the bulk-like region,

$$\langle \Theta(h) \rangle = \frac{1}{h} \int_0^{a\xi} \Theta(z) dz + \frac{1}{h} \int_{a\xi}^h \Theta(z) dz. \quad (13)$$

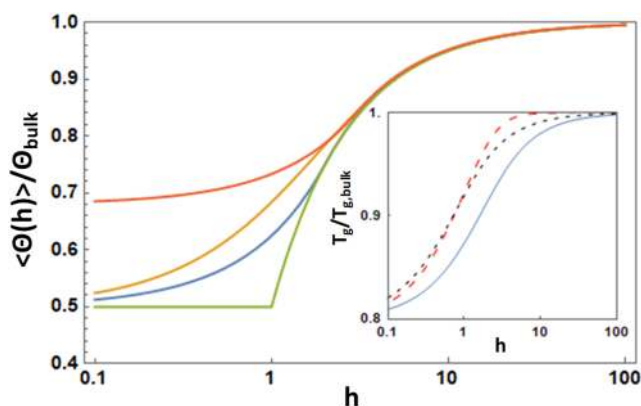


FIG. 6. Predictions of normalized mean film property vs log thickness (in arbitrary units) for a step function [formal layer model, Eq. (12), green curve], exponential gradient [Eq. (11), yellow line], and linear gradient [Eq. (10), blue curve], each with an amplitude $A = 0.5$ and $\xi = 1$. The orange curve is Eq. (10) with $A = 0.32$ and $\xi = 3$, demonstrating that the amplitude and range parameters cannot be deconvoluted without data for film thicknesses approaching the gradient size. Inset shows the effects of distinct gradient weightings on $T_g(h)$ for a mean film T_g computed from the exponential gradient equation [Eq. (11)]: blue solid curve and red dashed curve employ $\xi = 1$ and $A = 0.2$ with a linear arithmetic average [Eq. (9)] and a dynamically weighted average (as in Ref. 78), respectively; the black dotted line shows the linear arithmetic average with the range parameter adjusted ($\xi = 0.45$) to match the visual inflection point of the dynamically weighted average.

Since, by construction, $\Theta(z > a\xi) \cong \Theta_{\text{bulk}}$, this can be rewritten as

$$\frac{\langle \Theta(h) \rangle}{\Theta_{\text{bulk}}} = 1 - \frac{\delta\Theta}{h}, \quad (14)$$

where

$$\delta\Theta = \int_0^{a\xi} \left(\frac{\Theta_{\text{bulk}} - \Theta(z)}{\Theta_{\text{bulk}}} \right) dz \quad (15)$$

is a *constant* that quantifies the total “missing” Θ in the near-surface region. Thus, the normalized $T_g(h)$ [or any other mean-film property $\Theta(h)$] is expected, *as a mathematical and not physical matter*, to be an inverse power law in film thickness at large h —a simple form that often fits well experimental and simulation data^{2,3,6,9} (although it is only expected to hold for properties that obey linear arithmetic averaging over gradients). Hence, for z greater than $\sim 2\xi$, the detailed gradient shape information is lost (integrates out to a constant), rendering it mathematically impossible to distinguish between the different models based on whole film measurements above this thickness. Moreover, because this integral commonly convolutes the gradient amplitude and range, even for a given functional form, it is generally impossible to deconvolute A and ξ based on data in this thickness range (illustrated in Fig. 6).

Complicating matters further, a substantial body of work has demonstrated that whole film measurements commonly *do not* report on a linear arithmetic average over local gradients.^{8,78–89} Instead, each measured property involves a convolution of local gradients with a (typically nontrivial) weighting function that is technique dependent. Recent simulations and theory by one of us have

demonstrated that dynamical measures of T_g are generally weighted toward slower-relaxing regions, while quasithermodynamic measures of T_g are typically weighted toward regions with a higher contrast between liquid and glassy susceptibilities (temperature dependences) of the relevant thermodynamic property.⁷⁸ These weights commonly point in opposite directions. Moreover, they can sometimes be substantial enough in magnitude to account for qualitative alterations in apparent trends in the magnitude of interface effects with chemistry.¹²⁰

An example of the significance of weighting effects is shown in the inset of Fig. 6. Here, the $T_g(h)$ resulting from an exponential $T_g(z)$ gradient per Eq. (11) is computed using different weighting functions. First, we adopt a linear arithmetic average [Eq. (9)], a commonly assumed (albeit typically incorrect) scenario (blue line). Second, we apply the weighting function expected for *dynamical* measurements of T_g (red dashed line), which one of us previously derived in a general way⁷⁸ (Eqs. 22 and 23 in Ref. 78). The latter involves the material-specific fragility—assumed for simplicity here to be 100 everywhere in the film. For both cases, we ignore near-surface density gradients. One sees from Fig. 6 that these two weightings lead to substantially different $T_g(h)$ functions, with far weaker T_g reductions reported by the dynamical average than the linear average for all h . Comparison of the dynamically weighted T_g to a linear-arithmetic-averaged T_g with an alternate value of ξ selected to approximately match the visual inflection point of the former demonstrates that the alternate weighting qualitatively changes the *shape* of the curve, rather than simply shifting it to lower thicknesses. Other dynamical quantities are subject to still different weighting functions, e.g., Debye-Waller factors measured by quasielastic neutron scattering are weighted toward lower values (slower or stiffer regions).⁷⁹ These weighting effects may further be overlaid with instrument-specific sensitivities.

Evidently, even within the assumption of an arithmetic average, single-valued mean properties in the $h > 2\xi$ regime contain little or no information on the interfacial gradient form. Instead, system-to-system and measurement-to-measurement variability in the shape of the $T_g(h)$ curve in this regime predominantly reflects differences in the weighting function with measurement and chemistry.

The $h < 2\xi$ regime (roughly where the data become concave up in Fig. 6) in principle contains information on the gradient form, but here additional challenges arise. First, even neglecting weighting effects, Fig. 6 indicates that qualitatively distinct gradient functional forms can lead to film averaged properties that are similar in magnitude even in the ultrathin film regime; experimental uncertainties may render discrimination between such forms extremely difficult. Second, the inset of Fig. 6 shows that the $T_g(h)$ shape remains quite sensitive to the weighting-function even in this regime; a serious attempt to compare measurements to theory would require combining theory with formal averaging rules^{78,79} for the appropriate metrology to yield results germane for different measurements. Most seriously, for $h < 2\xi$, the gradients can be expected to begin to interfere or interact, and this may modify their form, range and/or amplitude. This point will cause an unrecoverable loss of information, as the integral in Eq. (14) will convert a dependence of Θ on both h and z to an h -dependent-only mean property.

The above issues seem analogous to the problem of inversion of scattering data, where one must posit a plausible real-space structure

and then verify that it is consistent with all available data. However, the above analysis indicates that $T_g(h)$ data are not good candidates for definitive discrimination between alternate proposed physical models. Indeed, even given experimental noise *only* it is very doubtful that one can distinguish between an exponential and linear T_g gradient (yellow and blue curves in Fig. 6, respectively), based on $T_g(h)$ data alone, even including data for ultrathin films and ignoring the important effects of nonlinear weighting and gradient overlap. The introduction of weighting effects, etc., will then render this task exceedingly difficult, perhaps practically impossible.

We thus believe that the common strategy of testing theories via comparison to the thickness-dependence of mean film T_g data requires a serious reassessment. A future focus on comparison to the $T_g(z)$ gradient, which contains rich physical information that is effectively lost at the level of whole film $T_g(h)$, would provide a much stronger starting point for comparison between theory and experiment. At the same time, we emphasize that aspects of mean-film experimental T_g measurements *other* than their thickness dependence can be theoretically valuable. For example, these measurements can be important in establishing the presence of interface effects on dynamics (although they cannot exclude them for a given system with asymmetric interfaces due to the gradient averaging effects noted above), in probing the dependence on details of the interface, and in ascertaining the dependence on rate or time scale of measurement (see the discussion of onset behavior above).

E. Dependence on interface type

Many of the trends discussed above are *qualitatively* general with respect to the nature of the interface. For example, simulations suggest that the double exponential form of the relaxation time gradient is quite robust to details of the interface (e.g., vapor vs solid).^{2,68,69,72,74,102,129} This, in turn, provides indirect support for the generality of the barrier factorization and power law decoupling effects. Much more work probing the generality of the power law decoupling relation described above, and the evolution of the intrinsic dynamical length scale and amplitude in Eq. (6) with thermodynamic state, is needed for diverse interfaces. However, there is already a rich picture of strong and important *quantitative* dependences on interfacial structure, chemistry of the liquid, and detailed nature of interactions; these dependences provide a promising avenue for confrontation of theory with empirical observation.

Simulation and experimental studies have led to a fairly comprehensive picture of these interface dependences, at least at a whole-film level. In general, softer interfaces and interfaces with weak attractions yield faster relaxation, while attractive hard structured interfaces yield slower relaxation. Rigid, pinned particle, rough surfaces created under the “neutral confinement” protocol (even in systems with only repulsive forces) lead to strong slowing down of interfacial dynamics. In contrast, for smooth wall surfaces, the dynamics are accelerated compared to the bulk.² Overall, these nonuniversal effects highlight the roles of surface corrugation,^{2,129} mechanical rigidity,^{19,45,44,148,149} and enthalpic interactions.^{19,122,149,150}

Simulations of bilayer films by one of us¹⁹ suggest the following combined dependence on most of the variables mentioned above.

As interfacial interactions interpolate between fully repulsive and strongly attractive, the thin film T_g exhibits a linear crossover from free-surface-like suppression to strong enhancement, with the magnitude of the latter enhancement depending on substrate softness. Substrate softness is quantified by its high-frequency (glassy plateau) modulus or the inverse of its Debye-Waller factor¹⁹ $\langle u^2 \rangle$, where $\langle u^2 \rangle$ is a measure of the size scale of high-frequency rattling within a regime of transient localization and exhibits an inverse relationship with the high-frequency shear modulus.^{151–154} The T_g dependence on interfacial attraction scales exponentially with the inverse ratio of the high frequency moduli of the confined to confining materials,^{19,75} i.e.,

$$\begin{aligned} \frac{T_g}{T_{g,\text{bulk}}} &= \frac{T_{g,\text{freestanding}}}{T_{g,\text{bulk}}} + AE_i \exp\left(-B \frac{\langle u^2 \rangle^{\text{confining}}}{\langle u^2 \rangle^{\text{confined}}}\right) \\ &\approx \frac{T_{g,\text{freestanding}}}{T_{g,\text{bulk}}} + AE_i \exp\left(-B \frac{G_\infty^{\text{confined}}}{G_\infty^{\text{confining}}}\right), \end{aligned} \quad (16)$$

where $T_{g,\text{freestanding}}$ is the T_g of a freestanding film of equal thickness, E_i is proportional to the interfacial attractive strength or work of adhesion, G_∞ is the high frequency relaxed dynamical modulus, superscripts of “confined” and “confining” denote values for the confined and confining materials, respectively, and A and B are material-specific constants. This trend leads to a “compensation” or “dynamic neutrality” value of the wall-fluid interaction for any particular value of the wall stiffness, via a criterion that is *not* the same as the condition of thermodynamic neutrality. Indeed, for stiff walls, equal fluid-fluid and fluid-wall attractions (thermodynamic neutrality) tend to result in substantially slowed near-substrate dynamics, à la the “neutral confinement” models. This lack of equivalence between thermodynamic and dynamic neutrality highlights the important role of surface mechanical rigidity and atomic-scale corrugation in slowing down motion even in the absence of strong liquid-substrate attractions. These simulation-based findings are qualitatively consistent with experiments, where hard substrates can, depending on their interactions with the confined fluid, yield a spectrum of behavior spanning from T_g enhancement to suppression, including dynamic “neutrality.”¹⁵⁰ Beyond specific trends, these results emphasize the need for theory to predict an important role for the relative high-frequency modulus or Debye-Waller factor of the confining material.

Whether interfacial dynamics is sped up or slowed down relative to the bulk appears to depend on additional factors beyond those discussed above. Specifically, this is suggested by experimental studies that point to an asymmetry of how the dynamical gradient responds to different interfaces, with a longer-range gradient commonly found at interfaces where relaxation is accelerated as compared to interfaces near which relaxation is slowed.^{17,20,21} The corresponding intrinsic length scale in the double exponential relaxation time gradient for solid rough surfaces appears to be shorter than for a vapor or smooth wall interface.^{14,62,63,138} While not extensively explored in simulation data for T_g and relaxation times vs position in supported films appear consistent with a shorter range near substrates where T_g is enhanced than near free surfaces where T_g is suppressed.^{124,149}

Finally, for solid surfaces, a variety of different experiments that probe relaxation *dynamics* over a range of microseconds to hundreds of seconds have attempted to extract the thickness of a layer of slowed down dynamics near a hard surface at temperatures *above* the bulk T_g .^{155–157} Conceptually, they are similar to the dynamical measurements on freestanding polymer films discussed in Sec. II A.^{106–108} Specifically, frequency-domain dielectric loss measurements on well-dispersed nanocomposites have been performed that employ large silica nanoparticles at sufficiently low loadings that the system can serve as a mimic of a thick supported film. An extracted characteristic time scale of the slowed down interfacial layer measured in the temperature range of $(1–1.3) T_{g,bulk}$ reveals a layer thickness of a few nanometers at high temperatures, which grows nearly *linearly* with cooling to ~ 6 to 8 nm at the bulk T_g .^{155–157} At the bulk T_g , the slowed down layer relaxation is by these measurements 10–100 times slower than in the bulk for glycerol and several short chain polymers. Surprisingly, this enhancement factor is nearly *constant* over a wide range of temperatures. Researchers using other methods⁹ (e.g., NMR^{158,159}) that probe shorter time scales than dielectric spectroscopy have reported that the near surface layer can become effectively vitrified on the experimental time scale, again highlighting the important role of probing time scale dependence in inferring the nature of interface modification of liquid dynamics.

Given the above findings, a definitive theory should at least qualitatively predict the dependence of dynamical gradients on the nature of an adjoining interface, including the role of its high frequency modulus, corrugation or topography, and liquid-substrate attractions.

F. Ultrathin films and gradient overlap effects

A qualitatively new physical issue arises for ultrathin films—how are dynamical gradients altered when they overlap? In principle,

this question can be probed in symmetric freestanding or capped films, though the majority of experiments have focused on more complex asymmetric supported films. This issue is of high intrinsic importance and practical relevance given that Fig. 6 indicates that it is not possible to discriminate between distinct theoretical scenarios based on mean-film data taken at thicknesses above this regime; moreover, many applications of interest involve domains of order 10 nm size that are likely within this regime. Nevertheless, this regime has received relatively little experimental study, likely due to practical difficulties. The existing modest body of data does not definitively establish a clear scenario for the phenomenology in this regime.

For freestanding polymer films, McKenna and co-workers employed a bubble inflation method to probe rheological response and deduce a *dynamical* glass transition down to the ultrathin limit.^{160,161} The T_g of polycarbonate (PC) films [Fig. 7(a)] only 3 nm thick was measured, and an extraordinary T_g reduction of 122°C was observed.¹⁶¹ Interestingly, the PC data suggest a roughly linear variation of ΔT_g in $\log(h)$ down to $h \sim 3$ nm. Figure 7(a) shows the PC data to be roughly consistent in functional form with data on thicker polystyrene films. On the other hand, polyvinylacetate (PVAc) does not show any T_g reduction. This remains a puzzle, which may result from nonuniversal aspects such as chemistry-dependence of the onset condition (if the PVAc onset time exceeds the measurement time scale) or experimental complications such as moisture uptake by this hygroscopic polymer (absorption of small molecule additives can sometimes suppress interfacial alterations in dynamics,^{53,117,120} an effect of interest in its own right that may also relate to variations in onset time scale).

The seeming lack of change of shape of the measured T_g shifts compared to thicker films in Fig. 7 may argue against strong gradient overlap effects beyond near linear additivity. This deduction would also seem to be consistent with the dye reorientation dynamic

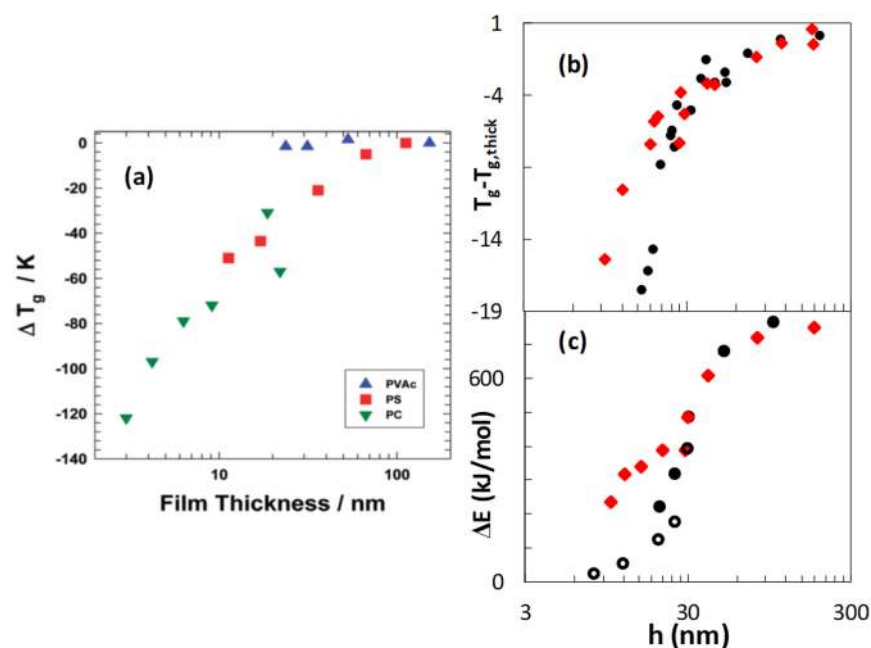


FIG. 7. (a) Thin film T_g from bubble inflation measurements for polyvinylacetate, polystyrene, and polycarbonate. Reproduced with permission from O'Connell *et al.*, *Macromolecules* **45**, 2453 (2012). Copyright 2012 American Chemical Society. (b) T_g suppression and (c) apparent low-temperature activation barrier reported by Zhang *et al.* for thin films of *N,N'*-bis(3-methylphenyl)-*N,N'*-diphenylbenzidine (TPD), a large, 6-conjugated-ring molecule.⁹⁵ Black circles are data for films on a poorly attractive substrate, while red diamonds are for films on a modestly attractive substrate. Filled symbols are based on rate-dependent T_g data from ellipsometry; open symbols are based on relaxation times inferred from dewetting experiments.

experiments discussed above on mobile layers in freestanding films,^{106,108} which found that the mobile layer thickness is *not* sensitive to film thickness down to 17, 7, and 24 nm for polystyrene (PS), poly(methyl methacrylate) (PMMA), and poly(2-vinylpyridine) (P2VP), respectively. Additional experiments on the same polymers for the supported film geometry (silica substrate) found essentially identical behavior as in freestanding films for PS and PMMA. Modest slowing down for P2VP films at a film-averaged level (expected given strong polymer-substrate attraction) was observed, but to leading order, the mobile layer at the vapor surface appears to be the same as in its freestanding analog. These findings suggest that any nonadditive coupling of the physics at the two vapor interfaces is weak at least down to these values of film thickness.

Early experimental work by Torkelson and co-workers also probed the ultra-thin-film regime by labeling a 14-nm thick near-surface layer of a supported film and varying the overall film thickness.¹⁰⁴ A substantial suppression in the free surface T_g of a thick film was found, consistent with an interfacial origin. As the film thickness is reduced below ~ 60 nm, the data provide evidence of a progressive weakening of this effect. This could be indicative of alteration of the near-free-surface-gradient via interaction with the near-substrate gradient. A potential complication is that the 14 nm domains comprise a large fraction (perhaps all) of the dynamical gradient such that the weighting effects discussed above may play a qualitative role. For the very thinnest films probed, where one might expect each interfacial gradient to fully span the film, the T_g shift becomes nonmonotonic, with an initial increase in this layer T_g followed by further apparent suppressions in T_g upon further thickness reduction. The potential importance of averaging effects seems especially plausible in this limit. Hence, these observations may suggest, but do not firmly establish, the existence of nontrivial dynamical gradient overlap effects for very thin films.

A mix of variable cooling rate ellipsometry and dewetting experiments have reported glass transition temperatures in supported small molecule films down to (in some cases) thicknesses of 8–10 nm.^{94,95} As shown in Fig. 7(b), T_g exhibits a progressive suppression with decreasing film thickness, qualitatively similar to the data of Fig. 7(a) for freestanding thin films, although the effect is of much smaller magnitude. The latter may result from some combination of distinct metrologies, differences in time scale, differences in the onset for these chemistries and metrologies, and substrate effects. The cooling-rate dependent T_g data were fit to an empirical Arrhenius form to obtain an *apparent* activation energy as a function of film thickness. Figure 7(c) shows that the extracted apparent activation energies exhibit a progressive reduction with decreasing film thickness. Results for a system on a more poorly interacting substrate exhibit an apparent extrapolation to zero of the apparent activation barrier at a finite value of film thickness. Dewetting data subjected to a similar analysis, especially if combined with the other data, suggest a sigmoidal turnover at low film thickness if this variable is plotted on a logarithmic scale. However, there is a substantial offset between the dewetting and ellipsometry data, and given the potential issues discussed above regarding metrology-dependence, there remains considerable uncertainty regarding ultrathin film behavior. A sigmoidal in $\log(h)$ behavior in supported films would also appear to qualitatively differ from the *dynamical* measurements on freestanding films of McKenna and co-workers¹⁶¹ and Paeng and Ediger,^{106–108} and perhaps also the viscosity measurements.¹²⁶ At

a minimum, these experimental contrasts indicate that ultrathin film T_g changes and dynamics may be nonuniversal, with a qualitative dependence on the confining interfaces and/or measurement technique.

Another important question for ultrathin films is whether dynamical gradients can become so severe that more than one distinct glass transition can emerge. Fakhraei and co-workers reported two distinct ellipsometric glass transitions in a narrow range of (small) supported film thicknesses if the polymer (P2VP) strongly adsorbs onto the solid substrate.^{140,162} Earlier studies of freestanding films by Pye and Roth reported the apparent presence of two distinct ellipsometric T_g 's in polymer films of extremely high molecular weight (M_w).¹⁶³ There, the higher T_g apparently corresponds to the T_g observed in non-high- M_w polymers and small molecule systems. The lower T_g thus far has been observed only in the ultra-high- M_w limit. In both the supported and freestanding cases, this “two- T_g ” phenomenon has only been reported for ultra-high molecular weight polymers and their relevance to the more general problem of dynamics in glass-forming liquids near interfaces is unclear. Moreover, their generality with regard to film and surface chemistry, as well as the question of whether this finding is unique to ellipsometry or present in truly dynamic measurements, is unknown.

Evidently, the limited experimental work in the ultrathin film regime does not definitively reveal how dynamical gradients behave when they span the entire film and can interfere. New simulation studies probing this question would be very valuable, along with more experimental data—particularly data providing insight into potential chemistry and metrology dependences in this regime.

III. THEORETICAL PROGRESS AND CHALLENGES

The simulation and experimental results surveyed in Sec. II point to key features of glassy dynamics near interfaces and in films against which theories can potentially be critically assessed. The most essential aspects that should be targeted from our perspective are summarized below. We refer the reader to Sec. II for discussions regarding the quantity and nature of evidence in support of each of these points. Each of these findings is in our view reasonably robust, but in many cases, further validating data will be beneficial.

One interface thick films: The problem of spatially heterogeneous dynamics in a one interface thick film (soft vs hard, rough vs smooth, and attractive vs not) is a very rich and theoretically more tractable initial target. It is of fundamental interest for its own sake and carries many of the interfacial and broken symmetry complexities of the thin film problem but without the extra complication of interface asymmetry and interaction of gradients from two surfaces. We believe that a definitive theory for such systems should predict at least the following key zeroth order features.

- The relaxation time empirically exhibits a double-exponential variation with distance from the interface, which implies that the underlying effective barrier gradient varies exponentially in space.
- The intrinsic range (not practical recovery of bulk behavior) of these gradients exhibits evidence of saturation or

near-saturation at low temperatures, even when bulk dynamics remain non-Arrhenius. At a minimum, simulations indicate that the temperature-dependence of this length scale grows *weaker*, rather than stronger, on cooling at low temperatures accessible to simulations.

- Strong fractional power law decoupling of the relaxation time relative to the bulk emerges beyond an onset condition with chemistry and relaxation-function dependences.
- Beyond the onset, local (film-averaged) dynamics obey a position-dependent (thickness-dependent) fractional power law decoupling relation due to the “barrier factorization” property.
- The relaxation time gradient is primarily of dynamical nature: structural alterations immediately *at* the interface may play an important role in *nucleating* the gradient, but *local* dynamics are not controlled *locally* by the structure within the gradient, and transfer of the relaxation time perturbation in the film is thus dynamical in nature.
- The amplitude, direction, and range of the dynamical gradient exhibit rich dependences on chemistry, interface type, and thermodynamic state.

Beyond the above core features, a complete theory should predict gradients in T_g , Debye-Waller factor, elastic modulus, and surface diffusivity and should provide insight into the role of intrinsic bulk dynamic heterogeneity.

Two interface thin films: Additional questions arise for ultrathin films that should be addressed by a complete theory. However, because the phenomenological understanding of this regime is presently poor, the precise predictions that should be made are less clear. Key questions include the following:

- How does the phenomenology for thick films change due to the presence of two interfaces and confinement in freestanding, supported and capped films?
- How do gradients interact in thin films with various boundary conditions?
- What are the conditions for vanishing of any bulk region of relaxation time, local T_g , and other dynamic properties in symmetric and asymmetric thin films?

A secondary task is to employ the theoretical understanding to make predictions for film-average properties, taking account of correct weighting of the local gradients.

In the remainder of this section, we discuss models and theories that have been employed to address elements of the above phenomenology. The problem is daunting since understanding activated glassy dynamics in the bulk remains an open challenge. At this time, there are no theories that capture all the rich phenomenology discussed in Sec. II. In many cases, the phenomenological picture described in Sec. II was not fully available at the time of theory development and improvements may thus be possible in light of this new phenomenological understanding. We consider only interfacial alterations of *equilibrium* dynamics. The theories discussed below vary tremendously with regard to their extent of development and application to experiments and simulations. This reality is reflected in the amount of discussion according to each approach, which should not be viewed as judgmental concerning future potential.

We note that multiple theories employ the symbol τ_0 to refer to a microscopic time scale that sets the elementary time of the activated alpha relaxation process. Though its value may vary modestly from model to model, it is expected to be always short (e.g., picosecond), and it is generally not central to the question of alterations in the longer-time structural alpha relaxation process near interfaces.

A. Theories based on a configurational entropy crisis

Beginning with Kauzmann,¹⁶⁴ the proposition that slow dynamics in glass-forming liquids is intimately linked to a reduction of configurational entropy with cooling has been a major thermodynamics-based hypothesis. Multiple theoretical frameworks invoke this scenario, but in different ways. Below, we discuss three approaches: Adam-Gibbs (AG) theory,¹⁶⁵ Random First Order Transition (RFOT) theory,^{166,167} and the “string” reformulation of AG theory.¹⁶⁸

1. Adams-Gibbs theory

Historically, much of the thinking regarding interface and nanoconfinement effects on the glass transition has been influenced by the Adam-Gibbs theory.¹⁶⁵ This scenario encodes two physical ansätze, which in their most general formulation are the following:

- (i) A chemically specific high-temperature activation free energy barrier $\Delta\mu$ (assumed to be a literal Arrhenius process and energy barrier in the original AG implementation) is *amplified* upon cooling due to an increasing degree of spatially correlated motion quantified by the average *number* of dynamical units required for a microscopic relaxation event: a “Cooperatively Rearranging Region” or “CRR.”
- (ii) The growing CRR mass scale or cooperativity number is driven in a simple inverse manner by a loss of configurational entropy on cooling.

This scenario is encoded in the AG equations,

$$\tau(T) = \tau_0 \exp\left(n \frac{\Delta\mu}{kT}\right) = \tau_0 \exp\left(\frac{\Delta\mu s_c^*}{kT S_c(T)}\right), \quad (17)$$

where n is the number of dynamical units that must cooperate to permit relaxation, $\Delta\mu$ is a high-temperature activation barrier, s_c^* is a critical configurational entropy required for relaxation, and S_c is the system configurational entropy. Empirical fits of Eq. (17) to bulk relaxation generally result in rather small values of n . While a CRR is often viewed as a compact spherical domain, it is not clear that this is consistent with small values of n . More generally, CRR size could depend on the number of cooperating units and fractal dimension D as $\xi_{CRR} \sim n^{1/D}$.

Two scenarios based on Eq. (17) seem relevant. First, interfaces or confinement modifies *mean* configurational entropy, which alters *mean* film dynamics, i.e.,

$$\langle \tau(T, h) \rangle = \tau_0 \exp\left[\frac{\Delta\mu s_c^*}{kT \langle S_c(T, h) \rangle}\right], \quad (18)$$

where the brackets are an average over a film of thickness h . This idea suggests that confinement-induced reduction of S_c should slow

down relaxation.^{1,51} Alternatively, free-surface-induced reduction of film-averaged density could enhance configurational entropy and accelerate dynamics.¹⁶⁹ A speculative alternative scenario might apply at the level of CRRs, with finite film size truncating their size [reducing n in Eq. (18)] and accelerating dynamics. This scenario can be encoded in an analog of Eq. (18),

$$\langle \tau(T, h) \rangle = \tau_0 \exp \left[\left\langle n(T, h) \right\rangle \frac{\Delta \mu}{kT} \right]. \quad (19)$$

Within these interpretations, there is no intrinsic invocation of a dynamical gradient of any kind—these perspectives posit effects at the level of the entire confined material.

A second alternative AG-like perspective is to introduce a correlation length that changes dynamics out to a distance from the interface that is proportional to the CRR size, ξ_{CRR} , which scales inversely with configurational entropy.^{104,170} The mean film relaxation time then reflects a spatial average over this local relaxation time (relaxation times, unlike other dynamical quantities, typically are expected to obey a roughly linear arithmetic average over gradients⁷⁸),

$$\langle \tau(T, h) \rangle = \frac{1}{h} \int_0^h \tau \left(\frac{x}{\xi_{CRR}} \right) dx = \frac{1}{h} \int_0^h \tau \left(\frac{x}{an^{1/D}} \right) dx, \quad (20)$$

where $\tau(x/\xi_{CRR})$ denotes a relaxation time that is a function of the distance from the interface reduced by the CRR size, h is a film thickness or domain size, D is the fractal dimension of the CRR, and “ a ” is a scaling factor.

It is unclear if the above two AG-based hypotheses can be mutually correct in a physically meaningful manner. In the first case, the relaxation time should be exponentially related to the degree of dynamic cooperativity, which changes with film thickness, via the AG relation. In the second case, cooperativity sets a length scale near an interface over which dynamics are altered, anticipating shifts in τ relative to bulk that should scale as in $n^{1/D}/h$.

The simulation and experimental results described in Sec. II, and recent work directly probing proposed AG CRRs in thin films,^{82,124,149} shed some light on the situation. The finding that dynamical gradients are usually the dominant origin of nanoconfinement effects on the glass transition generically points away from whole-film finite size alterations of configurational entropy as the leading order origin of these effects. Indeed, simulations and experimental results also indicate that the length scale over which bulk-like dynamics is recovered is generally *insensitive to film thickness*, at least for films sufficiently thick that these gradients do not substantially overlap.^{106,108,123} This also argues against a mean film-thickness-dependent shift in CRR size or configurational entropy as crucial. These considerations are evidence against the first scenario above. Moreover, AG theory makes no predictions for the form of the relaxation time gradient—arguably the central feature of the problem. At an even more fundamental level, the growing simulation evidence^{73,74,102,129,144,145} for a saturation or near-saturation of the intrinsic dynamic correlation length in a temperature range for which dynamics are non-Arrhenius poses a fundamental challenge to an AG approach, which invokes a growth in the cooperativity over the entire temperature range for which dynamics are non-Arrhenius.

The above discussion suggests that AG theory does not presently provide an empirically valid basis for understanding interfacial alterations of dynamics in glass-forming liquids.

2. Random first order transition theory

The Random First Order Transition Theory (RFOT) also posits that the growth in the apparent activation energy for relaxation upon cooling is due to a reduction of configurational entropy.¹⁶⁷ However, the underlying physical picture is distinct from the AG model, involving the concept of entropic droplets of nanoscopic size, and an unusual (not scaling as surface area) interfacial free energy between droplets of different microstructures or “mosaic patches.” This leads to a thermodynamic-like formulation analogous to nucleation theory, with the elementary dynamical object in the deeply supercooled regime being a compact droplet that grows with cooling and sets the *length scale* required for irreversible structural relaxation. This is in contrast to AG theory, where the CRR mass or cooperativity number plays the central role.

How the competing factors that determine the barrier in RFOT theory are quantified remains poorly understood and intensely debated. Briefly, the entropic droplet or cooperativity length scale is argued to scale in three dimensions as $\xi_d \propto S_c^{-3+b}$, where b is an “interface exponent,” and the relaxation time scales with this length scale as a power law, $\ln(\tau/\tau_0) \propto \xi_d^\gamma$, where γ is a different “dynamical exponent.”^{167,171} The net result, at the zeroth order, can be expressed as¹⁷¹

$$\ln(\tau/\tau_0) \propto (TS_c(T))^{-x}, \quad (21)$$

where $x = \gamma/(3 - b)$. RFOT predictions are very sensitive to the value of the exponent “ x ,” since its value controls the *functional form* of the temperature dependence of the barrier. There are different theoretical arguments⁶³ for x varying in the range of 1–2. However, recent analysis¹⁷¹ suggests that agreement of RFOT with observations requires $x \sim 0.5$ – 0.6 , much smaller values for which no theoretical basis presently exists.

There have been limited efforts to predict dynamics in one-interface thick films based on RFOT. Dynamics near a free surface have been argued to be massively sped up since half of an entropic droplet is missing.¹⁷² A central result is that the surface relaxation time obeys

$$\tau_{\text{surface}} \sim (\tau_0 \tau_{\text{bulk}})^{1/2}, \quad (22)$$

where τ_0 is a microscopic time. Effectively, the bulk barrier is reduced by a factor of 2 at the free surface, although the underlying physics remains determined by the same physical effects as in the bulk. This formula can give reasonable magnitudes for the massive speeding up at a vapor surface observed at the bulk T_g . However, there are problems with regard to its predicted temperature-dependence compared to the experiment, e.g., near surface-dynamics are much closer to Arrhenius over the observed temperature range,^{59,60,91,92} while Eq. (22) still predicts a super-Arrhenius variation.

A second result invokes additional assumptions about how enhanced mobility nucleated at an interface is transferred into the bulk. It emerges from an argument that the relevant length scale follows from an ideal mode coupling theory¹⁷³ (MCT) analysis at rela-

tively high temperatures. The central prediction is that the relaxation rate varies exponentially with distance from the interface,¹⁷²

$$\tau^{-1}(z) \approx (\tau_{\text{surface}}^{-1} - \tau_{\text{bulk}}^{-1})e^{-z/\xi_{\text{int}}} + \tau_{\text{bulk}}^{-1}. \quad (23)$$

This result is inconsistent with the double-exponential relaxation-time gradient phenomenology. Moreover, whatever the relevant intrinsic length scale is, an entropy-based scenario in general (and RFOT in particular) would seem to anticipate that it grows with cooling. This is in apparent conflict with the evidence for a weakening temperature dependence on cooling and (near) saturation of this length scale observed in simulations discussed in Sec. II. The functional form of Eq. (23) also does not correspond to the power law decoupling behavior observed in the recent simulation studies.⁷³

The phenomenology of Sec. II thus appears to challenge the ability of RFOT as currently formulated to capture alterations of glassy dynamics near interfaces and under confinement.

3. “String” model

The most extensively developed theoretical approach based on a configurational entropy perspective for the interfacial and confined glassy dynamics problem is a revised version of the second AG scenario discussed above. This perspective posits that the CRR of the AG theory has a one-dimensional “string” geometry composed of a relatively small number of particles,¹⁶⁸ which further serves as a correlation length setting the range over which near-interface dynamics recover their bulk value.¹²⁴ The strings are modeled as equilibrium polymers, leading to a mean string length that grows modestly on cooling. This approach predicts a saturation of the (string-like) CRR scale at very low temperatures (where dynamics are predicted to return to an Arrhenius temperature dependence), thus avoiding a true thermodynamic phase transition.

This approach again postulates a direct relationship between relaxation time and cooperativity at the film-averaged level, but with a functional form slightly different from the classic AG form,¹⁶⁸

$$\tau = \tau_0 \exp\left[\frac{n}{n_A} \frac{\Delta\mu}{kT}\right]. \quad (24)$$

Equation (24) differs from the first equality in Eq. (17) only via a normalization of the CRR scale by its value, n_A , at a crossover temperature T_A defined as the point where the relaxation time first becomes non-Arrhenius. Operationally, this framework treats $\Delta\mu$ as a high temperature activation free energy, which is assumed to vary linearly with temperature down to the glass transition. The model anticipates a dynamical gradient of range controlled by the string length, n . Douglas, Starr, and coworkers reported an empirical linear relationship between the practical (not intrinsic) length scale ξ_{rbulk} over which bulk-like relaxation times are recovered and n , which has been argued to support the above scenario.¹²⁴

We note that the algorithm employed to identify these strings has thus far been employed only at the level of bead-based models, and extensions of the string-based perspective to analyze other, very different, simulation models and lower temperatures would be valuable in assessing its generality. Of more direct relevance to the present issue, very recent work has indicated that the string-AG scenario does not predict interface effects on dynamics.

Specifically, it has been shown that the reduced cooperativity ratio n/n_A in Eq. (24) is only weakly altered in thin films.¹⁷⁴ Hence, alterations of thin film dynamics empirically *must be* dominated by changes in the temperature-dependent function $\Delta\mu$ with varying film thickness,^{149,174} a quantity viewed as the noncooperative component of an AG-like entropy description. This is a significant limitation, given that shifts in dynamics near interfaces apparently do not arise from the core cooperative configurational entropy physics, and the AG theory contains no prediction for $\Delta\mu$. Hanakata *et al.* suggested that $\Delta\mu$ could be modeled via classical transition state theory;¹⁴⁹ however, this has thus far not been shown to make any testable predictions for near-interface alterations in $\Delta\mu$. More generally, it is unclear that a thickness-invariant CRR scale is consistent with the basic AG framework.

For the above reasons, a compelling case for rationalizing interfacial alterations in glassy dynamics via string-like cooperative motion in an AG framework would require a parameter (both implicit and explicit)-free extension of the string detection algorithm [and thus Eq. (24)] to distinct glass-forming liquids, and development of a predictive physical model for the nonuniversal local barrier quantity $\Delta\mu$. Beyond this, the string scenario does not appear at present to predict multiple aspects of the phenomenology discussed in Sec. II, including exponential recovery of bulk-like barriers with increasing distance from the interface. Perhaps most significantly, if the intrinsic interfacial dynamic correlation length (nearly) saturates on cooling at a time scale for which dynamics are non-Arrhenius, as is suggested by recent simulation work, how can a growing dynamic length be responsible for the apparent growth in activation energy on cooling as envisioned by AG theory? Finally, can this scenario (or AG-based models in general) explain, in a parsimonious manner, the onset behavior of strong nanoconfinement effects upon cooling observed in simulation and experiment?

B. Free volume, dynamic heterogeneity, and percolation based models

We now discuss a class of models that have in common the idea that a minimal amount of “free volume” is required to achieve relaxation and diffusion. The definition of “free volume” has no accepted unique formulation.¹⁷⁵ Various ideas posit a deep connection between activated relaxation and some measure of steric crowding, available molecular space, and/or density.

Efforts to explain dynamics near interfaces using free volume theory have classically relied upon the proposition that the gradient in local dynamics reflects a corresponding gradient in local free volume or density.¹⁷⁶ Typically, some local version of the Doolittle equation is adopted,

$$\tau(z) = \tau_0 \exp[v^*/v_f], \quad (25)$$

where v^* is some critical specific volume locally required for relaxation and v_f is the free volume. Provided free volume is defined as a local structural or thermodynamic quantity, as has historically been the case, this scenario in a thin film context (sometimes termed a “free volume layer model”¹²³) would seem to conflict with the many simulation studies that find a lack of local correlations between dynamics on the one hand and structure and density on the other near interfaces of supercooled liquids.

In its more modern incarnations, some free volume theories presume that dynamic heterogeneity and percolation are central to glassy dynamics in films. Others argue for dynamic cooperativity of free volume in various ways or “mobile defects” that can unlock locally arrested regions. Here, we discuss recent progress from this class of perspectives.

1. Percolation of slow domains model

There is a long history of constructing phenomenological glassy dynamics models based on a binary description of a cold fluid consisting of nanoscopic “mobile” or “liquid” domains and “immobile” or “solid” domains. This includes the original marriage of the Doolittle free volume idea with percolation ideas by Cohen and Grest.¹⁷⁷ This perspective has been further developed with novel elements and applied to experiments by Long and co-workers.^{178,179} A distribution of domains of variable density and relaxation times is invoked. Initially, this is related to a static density fluctuation distribution determined by small scale thermodynamics, but elaborations allow for some time evolution. The bulk glass transition is assumed to be determined via site percolation of immobile domains. This phenomenological model does not aim to understand the mechanistic origin of local immobility since it adopts the empirical free volume expression.

In the initial work,¹⁷⁸ the fundamental idea was that as a film thins, the site percolation transition of slow domains changes from a 3-dimensional to 2-dimensional character. The focus was on films 20 nm or thicker where local interfacial effects that might change thermodynamic or structural properties are effectively absent, and explicit coupling of the 2 interfaces is presumed unimportant. Film-averaged properties, not the relaxation time gradient, were analyzed. In vapor interface films, the film-averaged relaxation time is proposed to be controlled by macroscopic site percolation of slow domains in the direction *parallel* to the film. Since the space-spanning percolation threshold increases with decreasing dimensionality, this leads to a decrease in T_g as the film thins. In qualitative contrast, for capped films with strongly adsorbing surfaces, it is postulated that the percolation aspect is fundamentally changed in such a manner that the film vitrifies when a finite fraction of slow domains connects the two interfaces over the *finite* length scale that defines film thickness. This is argued to occur at a *lower* percolation threshold than in bulk 3D, leading to an increase in the film T_g . In both cases, the model predicts that the film-averaged T_g shift varies as an inverse power law in film thickness with an exponent controlled by the 3d percolation correlation length, which numerically is only modestly larger than unity. Results for the form of thickness-dependent T_g shifts are consistent with measurements. However, the T_g spatial gradient falls off very slowly as a function of distance from the interface, specifically as an inverse *power law* with an exponent modestly larger than unity. As discussed in Sec. II, many simulations and some experiments suggest that this is not the form of the T_g gradient. Moreover, such a power law behavior is inconsistent with the observed *exponential* recovery of the bulk barriers with increasing distance from the interface that underlies the double exponential form of the relaxation time gradient and the detailed nature of the power law decoupling effect.

In subsequent work, the dominant relaxation time in films for different experimental probes and how it changes with film thickness and substrate were examined.¹⁷⁹ Of special interest was the

case of “intermediate” attraction strength between the liquid and substrate. Since T_g is envisioned to increase (decrease) for strongly (weakly) interacting interfaces, it was argued that $T_g(h)$ can become a nonmonotonic function of film thickness, first increasing as a film thins, and then decreasing in the ultrathin limit, in a manner reminiscent of experiments of Torkelson and co-workers.¹⁰⁴ Whether this happens is sensitive to chemistry. The “onset” question of the role of experimental time or frequency was also considered. For a vapor interface film, the model suggests that it is possible to observe faster dynamics relative to the bulk at higher frequencies, but no change at lower frequencies. This appears to be the opposite of what is observed in simulation and experiment where T_g shifts are small (large) if probed at high (low) frequency.^{91,94,130–132,140}

More recently, the free volume percolation model was modestly modified⁸⁶ and applied to analyze T_g changes near vapor and solid surfaces. The T_g spatial gradient again appears to be roughly an inverse power law in distance from the surface. Applications to polymer films suggest that the model can rationalize the magnitude of film-averaged T_g elevations near a substrate but does not properly capture T_g reduction near a vapor interface.

Overall, despite early successes for the form and direction of *film-averaged* T_g shifts in films (which we argue to be a poor theoretical discriminator), the free volume percolation approach either seems to disagree with key aspects of the phenomenology or has not yet addressed some of the central issues such as fractional power law decoupling of the relaxation time gradient.

2. Free volume string model

Recent work has constructed a model around the concept of string-like CRRs, but based on a *free volume* rather than entropy perspective.¹⁸⁰ It is proposed that a particle requires a sufficiently large “gate” between nearest neighbors to escape its cage. Invoking particle-spacing arguments at the mean density level, it is argued that above some particle volume fraction this process is, on average, not possible at a single particle level but requires many-particle cooperative motion. Based on an estimate of the number of cooperating particles needed to provide sufficient space for a tagged particle to escape its cage, a functional form for the dependence of the critical minimum number of cooperating particles as a function of volume fraction was derived,

$$N^*(\phi) \sim \frac{(\phi_V/\phi_c)^{1/3} - 1}{(\phi_V/\phi)^{1/3} - 1}, \quad (26)$$

where ϕ is the volume fraction, ϕ_V is the volume fraction at a postulated dynamic arrest condition, and ϕ_c is an onset volume fraction. Combining this with an estimate of the probability of N^* particles undergoing an irreversible motion yields a prediction for the relaxation time,

$$\frac{\tau}{\tau_0} \sim \left(\frac{\tau}{\tau_c} \right)^{N^*}, \quad (27)$$

where τ_c is “a typical liquidlike relaxation time at the cooperativity onset”¹⁸⁰ and τ_0 is a molecular time scale. Combining this with an activation model for τ_c yields the AG form, albeit *without* any direct connection to configurational entropy. Combining equations 26 and 27 with a constant thermal expansion coefficient provides a

mapping to temperature that yields the VFT relation. Two adjustable fit parameters enter: a “critical interparticle distance” for relaxation and a Vogel temperature T_0 where the relaxation time is presumed to diverge.

This model for bulk liquids was extended to thin films by assuming that a vapor interface simply *cuts off* the string length, progressively reducing the local “cooperatively number” as the interface is approached, leading to a gradient of relaxation time of the power law form,

$$\frac{\tau(T, z)}{\tau_0} = \left(\frac{\tau_{\text{bulk}}(T)}{\tau_0} \right)^{f(z/\xi(T))} \quad (28)$$

An analytic form for the effective exponent function $f(z/\xi(T))$ based on Fickian diffusion statistics is proposed, which numerically behaves very similarly to a simple exponential decay.

Unlike the AG or AG-motivated string theories, the above model provides a specific functional form of the variation of τ with distance from a free surface. Moreover, the derived form is in qualitative agreement with the observed double-exponential recovery of bulk-like relaxation time near a free surface. Equation (28) mathematically resembles the fractional power law decoupling relation of Eq. (1). However, as a consequence of the assumption that the temperature dependence of the key length scale $\xi(T)$ underlies non-Arrhenius relaxation in the bulk, the correlation length exhibits a diverging temperature dependence, $\xi(T) \sim \sqrt{\frac{T_c - T_0}{T - T_0}}$. This aspect does not seem consistent with the low-temperature fractional power law decoupling behavior observed in recent simulations nor with evidence for low-temperature saturation or near-saturation of the intrinsic barrier length.⁷³ On the other hand, the temperature dependence of the length scale above is rather weak at temperatures far above T_0 ; the authors of the model argued that this temperature dependence is not a major effect near the bulk T_g . We do note, however, that this form would at least appear to anticipate a strengthening of the temperature dependence of ξ upon cooling; this appears to be potentially at odds with the simulation observations that it weakens upon cooling.

Other questions also arise. To date, the model has not addressed the higher temperature regime probed in simulations discussed in Sec. II. How the two microscopic fit parameters impact the functional form and temperature dependence of the dynamical gradient, the question of factorization of the z and temperature dependences of the barrier, and fractional power law decoupling remain to be clarified. The proposed rearrangement scenario is evidently motivated by the string-like motions discussed above in the context of AG-string theory. However, simulations identifying these string-like excitations have reported that their size is fairly uniform in films, including near the vapor surface.¹⁷⁴ This may challenge the physical mechanism of ‘string CRR truncation’ at a vapor interface that underlies this model. The question of the generalizability of “string-like” CRRs beyond the simulated bead-based models where they have been observed thus far is also relevant to the generality of this framework.

In summary, the free volume string model appears to capture several salient features of the phenomenology of thin films, most notably the form of the dynamical gradient near a vapor surface, especially if the correlation length is nearly temperature-independent in a practical sense over the relevant temperature

range. However, there are several elements (the growing temperature dependence of the interfacial range on cooling and the string CRR truncation physical model) that do not appear to accord with phenomenology. Other aspects of the problem, such as the onset behavior and dependence on chemistry of the fluid and nature of the interface, have not yet been addressed.

3. Cooperative free volume model

Recently, White and Lipson proposed a “cooperative free volume model” (CFV) in which relaxation is posited to involve cooperative rearrangements in a manner reminiscent of AG theory,^{181,182} albeit with a theoretical basis in free volume rather than entropy concepts. This theory argues that free volume *cannot* be defined locally based only on the local density; instead, one needs to analyze the mean free volume within some cooperative radius about a central point. This idea (which is not explicitly incorporated in the theory at a local level to date) is proposed to be the origin of the lack of strong correlations between local density and local dynamics. The model employs mean free volumes computed from the Locally Correlated Lattice (LCL) model^{183,184} based *purely upon thermodynamic data*, rather than fit to a dynamical property as has been the standard for prior free volume models. The CFV model is motivated by earlier work that identified a phenomenological correlation between T_g and free volume in the bulk.¹⁸⁵ The approach is most directly relevant to modeling the isothermal density variation of relaxation rates in glass-forming liquids. To address isochoric and isobaric conditions, an empirical *power-law temperature-dependent function* is introduced, reminiscent of thermodynamic scaling approaches,^{186,187} to model the isochoric temperature dependence of relaxation times.

To apply CFV theory to films,¹⁸⁸ it is postulated that dynamic changes are driven primarily by near-interface alterations in free volume. A two-layer model is adopted, composed of a near-surface layer with altered free volume and dynamics, and a bulk-like domain with unperturbed properties further from the interface.¹⁸⁸ Dynamics are then argued to reflect a mean free volume averaged between these two domains. Ultimately, under an assumption that the difference between the near-surface and bulk free volume is constant, the mean film dynamics are given by¹⁸⁸

$$\ln \tau = \ln \tau_{\text{ref}} + \frac{(T^*/T)^b}{(V_{\text{free}}/V_{\text{hc}})_{\text{bulk}}^0 + (T - T^0)(\alpha V/V_{\text{hc}})_{\text{bulk}}^0 + (\delta_{\text{free}}/h)} \quad (29)$$

Here, $(T^*/T)^b$ is an *empirical* power law, where b may be determined by collapsing a set of bulk relaxation data plotted as isotherms against inverse free volume, and T^* is read from the slope of the resulting single line. The first two terms in the denominator are a linear approximation to the full LCL model prediction of the temperature dependence of the ratio of free to hard core volume, with $(V_{\text{free}}/V_{\text{hc}})_{\text{bulk}}^0$ denoting its value at the reference temperature and the second term describing its temperature dependence. If one sets δ_{free} to zero, Eq. (29) is an approximate form of the CFV/LCL description of the bulk relaxation time. Alterations to dynamics in thin films are thus encapsulated in the term δ_{free}/h , where h is the film thickness and δ_{free} is an adjustable parameter interpreted as quantify-

ing the extent of free volume enhancement in the near-surface layer. Equation (29) can thus be written in terms of the bulk relaxation time as

$$\ln \frac{\tau}{\tau_{ref}} = \frac{1}{[\ln(\tau_{bulk}/\tau_{ref})]^{-1} + (T^*/T)^{-b}(\delta_{free}/h)}. \quad (30)$$

Equation (29) provides good fits¹⁸⁸ of polymer film-averaged relaxation time data down to $h \sim 10$ nm. Most recently, Debot *et al.* shown that, after fitting the bulk parameters to bulk temperature-dependent dynamics and fitting δ_{free} to a single thin-film temperature, Eq. (29) can then predict thin film dynamics over at least a modest range of temperatures near the fit temperature.¹⁸⁹ Because free volume near a tagged particle close to the surface is viewed as reflecting an average *equilibrium* density within some distance of a particle, the model is expected to break down for films sufficiently thin that there is no bulk region.¹⁸⁸ The authors estimated that this occurs for film thicknesses around 10 nm for the poly(4-chlorostyrene) systems against which they compared their predictions.¹⁸⁹

The CFV model also predicts via Eqs. (29) and (30) that mean-film relaxation times will become less thickness dependent with increasing temperature.¹⁸⁹ For the P4CLS experimental system to which they compare, this prediction is in quantitative agreement with the data. We note that that these data extend only up to relaxation times of ~ 0.1 s, and given the conflicting data on the onset condition discussed above, it is not clear to us whether or not they are past the onset condition for strong nanoconfinement effects for this system—it is plausible that they may be in a higher-temperature regime in which interface effects have not realized their limiting low-temperature behavior. Nevertheless, this appears to represent potential progress toward a prediction of onset behavior from the CFV model. Further tests explicitly comparing predictions to empirical onset behavior in experimental and simulated systems for which an onset has been clearly observed would be of great value.

Overall, the CFV model presents a potentially promising path forward for free volume approaches to thin film dynamics. It has been compared to experiment more extensively than the majority of theories in the field. Prediction of a weakening of effects on relaxation times at higher temperatures is a promising qualitative success. Further assessment of the core ideas requires its generalization to directly treat spatial relaxation time gradients as well as the ultra-thin-film limit and other observations discussed in Sec. II. These extensions are critical to validating or falsifying the theory given the limitations, discussed above, of mean-film-property data in the thick-film regime in discriminating between distinct theoretical predictions. Such extensions would also enable testing against the double-exponential relaxation time behavior and exponential T_g gradients near simulated surfaces, as well as the power law decoupling effect. It would also enable a clearer assessment of whether the CFV model captures the strong phenomenological disconnect between local structure and local dynamics near interfaces.

4. Stochastic fluctuating mobility model

For bulk glassy dynamics, there is a long history of constructing phenomenological rules-based stochastic models of relaxation. “Dynamic facilitation” models have been extensively pursued

within this literature.¹⁹⁰ They generally emphasized the space-time dynamic heterogeneity of a coarse-grained mobility field with postulated evolution rules that are not rooted in explicit connections of mobility to structure or thermodynamics. To date, these dynamic facilitation models, which have been widely explored in the bulk, have not generally been extended to treat dynamics near interfaces and in thin films under equilibrium conditions.

Motivated by issues in polymer thin films, Tito, Milner, and Lipson^{191–193} created a phenomenological “limited mobility” (LM) model that shares some high level features with the dynamic facilitation picture but with different motional rules and elementary dynamical objects. The model consists of a Monte Carlo simulation of a lattice fluid in which sites are classified into 3 distinct states: “dense,” “dormant,” and “mobile.” Dynamical rules are constructed such that sites can swap or change states with assigned probabilities. Crucially, conversion from dormant to mobile free volume states requires an adjacent mobile free volume site (reminiscent of dynamic facilitation or kinetic Ising models¹⁹⁰), leading to clustering of mobile free volume. These states and dynamical rules are interpreted in a free volume scenario, wherein “dense” sites lack any free volume, “dormant” sites possess free volume that is insufficiently localized to immediately permit relaxation, and “mobile” sites possess sufficiently localized free volume so as to present an effective defect into which a particle can diffuse. These interpretations provide a physical rationale for its three-state nature. The model involves several parameters that are not deduced based on a microscopic analysis, including the fraction of sites possessing free volume (which for films is implemented via an equilibrium between dense and dormant sites) and the local rates of mobile-to-dormant and dormant-to-mobile switching. Ultimately, the overall mobility is quantified based on the mean fraction f of sites that are mobile. In the bulk, the model exhibits a second order dynamic phase transition at *finite* temperature, corresponding to a parameter-dependent condition at which $f = 0$. The transition involves a power-law divergence of the spatial dynamic heterogeneity length scale.

The LM model has been applied to supported thin films by manually imposing a fixed layer of mobile sites at a free surface, and a fixed layer of dense sites at a substrate, with correspondingly modified dynamical rules for swaps with the surface and substrate layers. This was shown to lead to an equilibrium profile of mobile free volume fraction, with an approximately *exponential* variation with distance from the interface. Given that f appears to us to be most closely related to a free volume fraction, the most natural basis for comparison would then be to assume $f \sim v_f$ in Eq. (25), suggesting $f \sim -\ln(\tau)$. Adopting this results in an exponential variation of v_f with distance from the interface, which could potentially agree with the observed double-exponential variation of relaxation time found in molecular dynamics simulations discussed in Sec. II. Moreover, this theory predicts a shorter interfacial dynamical range near substrates where mobility is reduced than near free surfaces, in qualitative accord with the phenomenology described in Sec. II. On the other hand, the model predicts a power law divergence of the interfacial range as the bulk critical condition is approached, with this divergence tracking a corresponding divergence of the bulk correlation length of dynamic heterogeneity. This feature appears to be inconsistent with simulation evidence^{73,74,102} for a saturation or near-saturation of the intrinsic dynamical length scale.

Other aspects of the phenomenology (e.g., power law decoupling, detailed interface dependences, and onset behavior) remain to be addressed. Given the current model interpretation in terms of local free volume, the question of whether this approach is consistent with the observed lack of strong correlations between local dynamics and structure in thin films seems unsettled, as is whether/how the states and dynamical rules implemented within the model relate to microscopic processes in glass-forming liquids.

C. Elastic activation models and elastically cooperative nonlinear Langevin equation theory

In bulk glass forming liquids, a family of “elastic activation models” have been developed over many decades.¹⁹⁴ They have a qualitatively different character than the frameworks discussed above, since the elementary local structural relaxation event is argued to strongly couple to the longer-range collective shear elasticity that generically emerges in cold viscous liquids. The basic scenario seems akin to solid state physics phenomena such as interstitial diffusion in crystals, and the intuitive picture is that deeply supercooled liquids are “solids that flow.”^{195,196}

1. Shoving model

At present, the most widely discussed elastic model is the “shoving model” of Dyre.^{195,196} Achieving a compact activated rearrangement (of unknown molecular nature phenomenologically modeled by an “inner” energy barrier E_A) is envisioned to require the local creation of a small amount of extra volume, V_c (constant, but of unknown magnitude). The latter is argued to be realized via a spontaneous elastic fluctuation associated with a long range (inverse power law) strain field outside the inner region, which is computed using continuum linear elasticity theory. This results in an additional “outer” barrier. The energy scale of the latter is set by the relaxed temperature-dependent plateau dynamic shear modulus, $G'(T)$, which grows on cooling. The shoving model postulates that this “far field” elastic barrier dominates at low temperatures, with the non-Arrhenius aspect of the relaxation time controlled by $G'(T)$ schematically as

$$\tau_{\text{bulk}}(T) \approx \tau_0 e^{\beta E_A + \beta G'(T) V_c}. \quad (31)$$

We are unaware of work that has employed this model to treat interfacial dynamics or thin films. However, since the physical picture involves a long range elastic strain field, the presence of an interface or of confinement would presumably strongly modify the effective barrier by cutting off and perhaps distorting the strain field. This can result in a novel mechanism for modifying the structural relaxation process that could be important even *far* from the interface. Such an elastic model scenario has motivated the development by one of us of a microscopic force-based theory, the Elastically Collective Nonlinear Langevin Equation (ECNLE) theory.^{96,197}

2. Elastically cooperative nonlinear Langevin equation theory

ECNLE theory is a predictive approach for activated single particle motion that qualitatively extends the earlier nonlinear Langevin equation (NLE) theory. The NLE theory predicts how stochastic single particle trajectories are affected by dynamical *local*

caging constraints quantified solely from knowledge of the equilibrium pair correlation function, $g(r)$, or static structure factor, $S(k)$. This information is encoded in a “dynamic free energy,” $F_{\text{dyn}}(r)$, where r is the particle displacement from its initial zero-time position. The negative gradient of the dynamic free energy determines an effective force on a moving particle, which enters a stochastic nonlinear Langevin equation that can describe large amplitude local hopping.^{198,199} In the more recent ECNLE theory,^{96,197} the hopping event is coupled to longer range collective elastic displacements of all particles outside the cage. Construction of the displacement field is motivated by the shoving model idea¹⁹⁵ but differs in that a particle-level Einstein glass framework is adopted. Importantly, the amplitude of the long-range displacement field and its net energetic cost that determines the elastic barrier are quantified in a predictive manner by the cage scale dynamic free energy. Hence, although the scale-free collective displacement field is relatively “long range,” the elastic barrier associated with its integrated consequence is determined by the properties of the local cage dynamic free energy (jump distance and local harmonic stiffness) and hence the packing structure. Overall, the total activation barrier is thus the sum of two deeply interrelated, but distinct, barriers—a local cage contribution and a longer-range collective elastic contribution. The former varies weakly with temperature per a noncooperative hopping process, while the latter is strongly temperature and density dependent, encodes the collective aspect of relaxation, and dominates growth of the relaxation time in the deeply supercooled regime.

Bulk ECNLE theory has been quantitatively confronted, often with no adjustable parameters, against relaxation time data in colloidal suspensions, molecular liquids, and polymer melts.^{96,197,200,201} Chemical complexity is *a priori* handled by mapping the real thermal liquid to an effective temperature-dependent hard sphere fluid that by construction exactly reproduces the experimentally known equilibrium dimensionless compressibility (dimensionless amplitude of long wavelength density fluctuations) of the real liquid. This mapping implies that, at the zeroth order, the form of the theory is quasiuniversal. There are no relaxation time divergences at finite temperature or below random close packing. Quantitative calculations accurately capture the relaxation time of hard sphere fluids over 5–6 decades and over 14 decades for nonpolar molecular liquids.^{96,197} Extension to polymers is based on a Kuhn segment model.^{200,201}

ECNLE theory has been generalized and extensively applied to interfacial and thin film dynamics over the past 5 years. A minimalist model is adopted that focuses *solely* on dynamical effects, in the specific sense that changes of thermodynamics and pair structure near an interface are presumed to be secondary effects which are ignored in the leading order analysis to date.^{85,88,202–205} Note that this is not a phenomenological “dynamic facilitation”¹⁹⁰ model type of description since the kinetic constraints that determine activated trajectories are still directly related to effective forces which *are* constructed from knowledge of equilibrium packing correlations [e.g., $S(k)$]. It is via the latter that nonuniversal chemistry, thermodynamic state, and interface type effects can modify physical behavior in the theory. The challenge then is to construct a dynamic free energy, $F_{\text{dyn}}(r; z)$, and elastic displacement field as functions of distance (z) from an interface. To date, three physical mechanisms by which dynamics are modified near an interface are included in the theory. (1) Within a

cage radius of the interface, a particle loses nearest neighbors, which are replaced by vacuum or solid surface. This changes the caging constraints for particles very close to the interface and nucleates a dynamical gradient.⁸⁵ (2) This surface-induced modification of caging constraints is transferred over longer distances into the film, reflecting the physical idea that particles closer to the vapor interface that are within the cage of a tagged particle in turn exert weaker dynamical constraints on it. This transfer is implemented in a bootstrapped manner, whereby constraints experienced by particles in layer j are influenced directly by the underlayer $j - 1$.²⁰⁴ (3) The collective elastic barrier is modified in a spatially dependent manner in two distinct ways.^{85,205} First, the magnitude of the elastic barrier depends critically on the particle jump distance and localized state stiffness which set the displacement field amplitude and elastic barrier energy scale, respectively. These quantities follow *directly* from the dynamic free energy at the cage scale and both become smaller as a vapor interface is approached. Second, the contribution of all the elasticity-deformed particles outside the cage requires a spatial integration out to rather large distances. Since the displacement field is cut off at a vapor (or rigidly pinned hard surface), this longer range effect also reduces the elastic barrier. The resulting cage and elastic barrier spatial gradients are strongly coupled. At a vapor interface, all three effects speed up dynamics and reduce cooperativity, and all three are intimately related.

Initial work^{85,88,202,203} addressed only freestanding films and did *not* take into account effect (2). Multiple *film-averaged* properties of molecular and polymer films (e.g., T_g shifts, mobile layer thickness, surface diffusion constant, dielectric loss spectra, and some quasithermodynamic properties) were quantitatively determined and shown to reasonably well describe experiments. However, although the decoupling and barrier factorization (fractional power law decoupling) effects were predicted,²⁰³ two fundamental aspects of the dynamical gradient were *not* captured: the double exponential form of the relaxation time gradient and the underlying exponential spatial variation of the decoupling exponent. Over the last year, the physical consequences of point (2) have begun to be worked out with a focus on thick films and a vapor interface.^{204,205} Key generic aspects of this advance are summarized below and compared to the empirical phenomenology, along with a discussion of new testable predictions.

The *caging* component of the dynamic free energy varies nearly exponentially with distance from the interface as a consequence of effect (2), and in a manner such that the dependence on distance from the interface and the dependence on temperature or volume fraction effectively *factorize*

$$F_{\text{cage}}(r, z; T) = F_{\text{cage}}^{\text{bulk}}(r; T) + e^{-z/\lambda} \Delta F_{\text{cage}}(r; T). \quad (32)$$

Here, $\Delta F_{\text{cage}}(r; T) \equiv F_{\text{cage}}^{\text{surface}}(r; T) - F_{\text{cage}}^{\text{bulk}}(r; T)$ is the *difference* between the caging dynamic free energy of the first surface layer ($z = 0$) of interest and in the bulk, and the *constant* decay length $\lambda \sim 1.4$ particle diameters. This behavior imparts *both* a roughly exponential spatial variation of *all* the key features of the dynamic free energy required to compute gradients of the transient localization length, barriers (local and most of the collective elastic), structural relaxation time, shear modulus, etc., *and* an invariance to leading order of the *ratio* of these quantities in the film to their bulk analogs

to changes of thermodynamic state (i.e., the factorization property discussed in Sec. II). Although the penetration length at the most fundamental level of the caging component of the dynamic free energy is constant, in practice the *effective* penetration length is predicted to be both property and interface specific. The precise nature of the interface enters via the first layer, where dynamical constraints can be weakened, softened, or hardly changed (e.g., vapor, pinned rough solid, or smooth hard wall, respectively²⁰⁴). Numerical calculations for the hard sphere fluid and molecular and polymer liquids have been performed.^{204,205}

For a thick film with a vapor interface, the theory makes multiple general predictions relevant to the phenomenology of Sec. II. First, as one expects physically, the collective elastic barrier is more strongly modified by the interface and perturbed to larger distances into the film, than its local cage analog. However, since the dominant effect of an interface on the local and elastic barriers involves the same caging component of the dynamic free energy, the *total* barrier follows (to a good approximation) an exponential spatial variation as expected from Eq. (32). Numerical calculations find that the bulk total barrier is not recovered until ~ 10 particle diameters from the vapor interface. Second, a near factorization of the z and temperature/density dependences of the total barrier follows. This implies that fractional power law decoupling is predicted, with an exponential variation of the z -dependent exponent, in qualitative accord with the simulation.⁷³ Third, a relaxation time gradient of a double exponential form, characterized by a nearly constant intrinsic length scale [$\xi \approx 3$ particle diameters in Eq. (6)] is predicted. Note that this ξ is nearly but not exactly temperature independent, in contrast to λ in Eq. (32) which is temperature independent and quantitatively smaller than ξ . Fourth, the gradient $T_g(z)$ normalized by the bulk T_g is predicted to be very weakly dependent on the vitrification criterion (varying from 100 ns to 100 s, beyond any onset threshold for this theory), which was analytically shown to be another consequence of barrier factorization. This result provides a possible additional theoretical basis, beyond chemistry and metrology dependence of the onset, for the puzzling finding discussed in Sec. II that *normalized* T_g gradients measured in simulation and experiment over vastly different time scales are often in close accord.

The theory predicts that decoupling applies over an enormous number of decades of relaxation time, with an “onset” occurring at very short times of ~ 10 ps. The latter time scale appears to be consistent with simulations of translational dynamics in bead-based models,^{2,73,114,124} but experimental systems may have much delayed onset times that the theory does not presently capture. This may not be a failure of the underlying dynamical ideas but rather may indicate that relevant nonuniversal aspects are not fully captured by mapping to an effective hard sphere fluid. More study of this key issue is needed.

ECNLE theory for a vapor interface thick film has made other testable predictions relevant to both simulations and experimental materials. Quantitative aspects (including temperature dependences) depend on chemically specific features such as the liquid equation-of-state and bulk fragility. Selected examples are as follows,^{204,205} (i) The degree of relaxation acceleration at the surface [amplitude A in Eq. (6)] grows exponentially with increasing packing fraction or decreasing temperature. (ii) A consequence of (i) is that the mean interfacial layer thickness of *practical* enhanced

mobility, given by $L_{int}(T) = \xi \ln A(T)$ to leading order, is rather large at the bulk T_g , ~ 6 to 12 nm depending on molecule or polymer chemistry. This length scale decreases roughly linearly with heating. (iii) The dynamic plateau shear modulus varies exponentially with distance from the interface, being smaller by a factor of ~ 3 to 4 at the vapor surface, and recovering its bulk value ~ 6 particle diameters into the film. A crude estimate of a film-averaged Young's modulus as a function of film thickness is in reasonable agreement with simulation and experiment. (iv) Quantitative predictions for the position-dependent relaxation time indicate that its temperature dependence strongly weakens upon approaching a vapor interface, with bulk behavior not attained until ~ 12 particle diameters from the surface. (v) The top two layers of a thick film are predicted to remain in equilibrium down to $\sim 80\%$ to 85% of the bulk T_g . This result appears to be qualitatively consistent with the experiments of Paeng and Ediger,^{106–108} is relevant to greatly enhanced surface diffusion,^{59,60} and seems consistent with a key criterion for the formation of ultrastable glasses.^{57,58} (vi) The functional form of the normalized T_g gradient is directly related to the barrier factorization and barrier reduction physics and is predicted to be

$$\frac{T_g(z)}{T_{g,bulk}} = \frac{\Gamma}{1 + \frac{\Gamma-1}{\sqrt{1-\varepsilon(z)}}}, \quad (33)$$

where $\varepsilon(z)$ is the ratio of the total barrier at location z to its bulk analog per Eq. (2). The nonuniversal dimensionless parameter Γ is the ratio of the temperature at the dynamic crossover to the deeply supercooled regime to the bulk T_g , which is ~ 1.2 to 1.4 for experimental molecular and polymer liquids.^{103,138,139,190,197} Relative to unity, smaller (larger) values of this parameter suppress (enhance) both the magnitude and spatial range of the T_g -gradient. Conceptually, Eq. (33) connects the normalized vitrification temperature gradient to the barrier factorization property and reduction factor in Eq. (2) and is qualitatively consistent with the empirical equation (4). (vii) In practice, numerical calculations reveal that, to a good approximation, the T_g gradient is of an exponential form in z , which is a direct consequence of the exponential variation of the barrier with distance from the surface. Numerical calculations of $T_g(z)$ appear consistent with the simulations of Fig. 5 with regard to the functional form, degree of suppression at the surface, and spatial range for a thick film with one vapor interface. Quantitatively, in practice, large and long range gradients of $T_g(z)$ are predicted. For example, for polystyrene a ~ 100 K reduction of T_g at the surface is found, with recovery to within 1%–2% of the bulk T_g not achieved until ~ 30 to 40 nm or Kuhn segment diameters from the interface. (viii) A spatially averaged glass transition temperature associated with simple weighting of the T_g gradient from the surface ($z = 0$) to a depth of " Δ " in the thick film was studied, $\langle T_g(\Delta) \rangle \equiv \Delta^{-1} \int_0^\Delta T_g(z) dz$. This quantity is a crude surrogate for a film-thickness-dependent T_g if dynamical gradient overlap effects are weak or absent, in the spirit of the calculations leading to the inset of Fig. 6. Calculations for polystyrene find that it does not recover the bulk T_g value until $\Delta \sim 50$ or more Kuhn segment diameters from the interface.²⁰⁵

Most of the above results are *directly* related to the predicted double exponential form of the relaxation time gradient and fractional power law decoupling effect.²⁰⁵ Moreover, they follow almost entirely as a consequence of the recently introduced^{204,205} physical

effect (2), which as mentioned above strongly modifies in a spatially resolved manner *both* the local cage and collective elastic barriers. The explicit cutoff of the elastic displacement field is a relatively minor effect compared to interface-induced changes of the cage-scale-determined displacement field amplitude and localized state stiffness. However, at large enough distances from the interface, the elastic displacement field cutoff effect does become important, resulting in a low amplitude tail of the barrier gradient that approaches its bulk value as $\sim z^{-1}$.²⁰⁵ This implies that the logarithm of the alpha time gradient approaches its bulk thick film limit as an inverse power law of distance with the interface. Testing this result with the simulation will be challenging given issues surrounding statistical sampling and computer time scale limitations, but in principle it is possible.

Many issues have not yet been addressed by ECNLE theory, including thick films with diverse solid substrates and some observations discussed in Sec. II. Since the fundamental theoretical ideas are not specific to a vapor interface,²⁰⁴ one can expect (and preliminary work finds²⁰⁶) that the generic behaviors qualitatively hold for solid surface thick films. Extension to treat finite thickness films and bilayers is in progress. The former systems require addressing how gradients at two surfaces interfere, while the latter involves understanding how the elastic displacement field extends between two glassy materials of different dynamic shear stiffness. The influence of the detailed nature of the liquid-interface structure (e.g., adsorption) also remains to be addressed.

IV. OPPORTUNITIES AND CHALLENGES

It is evidently possible to theoretically predict or rationalize, via diverse physical perspectives, the coarse zeroth order finding that proximity to an interface or confinement to the nanoscale alters activated glassy dynamics. However, a focus on the thickness-dependence of T_g for individual chemical systems seems to be, as both a mathematical and practical matter, of little value in discriminating between distinct theories. Comparison to the microscopic phenomenology—particularly the spatial form of the relaxation time near interfaces, its onset and temperature dependence, the decoupling phenomenon, T_g gradients, and lack of correlation with local structure—is therefore critical to assessing which physical ideas genuinely reflect the real-world phenomenology. The current state of theoretical understanding of the problem, viewed through this lens, can be briefly summarized as follows.

At present, no purely entropy-based theory predicts near-interface alterations in dynamics in a manner that accords with the observed phenomenology. Instead, there appear to be significant inconsistencies and/or predictive shortcomings. Whether these problems can be remedied is unclear. Classical free-volume layer model approaches are not consistent with the basic physics of the phenomenon revealed by simulations. More modern free volume based approaches that combine dynamic heterogeneity and percolation concepts,¹⁷⁹ string-like particle motion,¹⁸⁰ cooperative free volume dynamics,¹⁸⁸ or free-volume-motivated dynamic-facilitation-like ideas¹⁹² make some predictions in accord with phenomenology. However, in all of these cases except the third (the cooperative free volume theory), some predictions seem to be inconsistent with the phenomenology. Additional theoretical development that allows comparison to far more elements of the rich

phenomenology described in this article (and potentially addressing any known inconsistencies) is necessary to validate or falsify these approaches. The force and particle level elastically cooperative nonlinear Langevin equation theory,^{96,197} which is built on coupled cage scale activated hopping and longer range collective elastic fluctuation, predicts a large portion of the observed phenomenology for thick one-interface films, including (to a good approximation) fractional power law decoupling, exponential variation of activation barriers near the surface, the barrier factorization property, and the double exponential relaxation time gradient.^{204,205} Given its microscopic basis, connections to chemically specific aspects enter naturally. However, it has not addressed some of the key aspects of the phenomenology nor been fully developed for diverse hard interfaces and finite thickness films, though efforts in these directions are underway.

Our review of progress in this field also points to several critical advances that we believe are required to develop a predictive understanding of near-interface alterations in dynamics and properties. We close by stating the most pressing ones, in our opinion.

1. Efforts at theoretical validation should move away from comparison with relatively thick film-averaged $T_g(h)$ data. Focus should be on comparison to highly resolved dynamical gradients (e.g., T_g , relaxation time, viscosity, and diffusivity) as determined from simulation. Comparison to experimental data in ultrathin films where gradient-interaction effects may become very important should be prioritized over comparison to data in the thick-film limit. However, as discussed above, numerous issues complicate the interpretation of mean-film data even in the ultra-thin-film limit; comparison to experiments that report on distributions of properties within the film should therefore be of high priority. These comparisons should also include the chemical and interface dependences of the dynamical gradients.
2. Experimental efforts should focus on detailed measurements and the development of improved metrologies accessing the types of data described in point 1.
3. Multiple nontrivial phenomenological aspects of the free-surface dynamical gradient are now known, including exponential variation of the effective barrier and local T_g near the surface, fractional power law decoupling, (near) saturation of the intrinsic correlation length, double exponential form of the relaxation time gradient, and a nontrivial onset condition. Prediction of these observations should be a standard test of any theory.
4. A much better understanding of the onset condition and its implications, including dependences on relaxation function and chemistry, is an urgent matter. Onset physics may account for much of the variation in apparent strength of nanoconfinement effects observed between distinct chemistries and experimental probes. Progress in this direction should also help clarify the connection between experimental and simulation studies.
5. The development of unified theories that address bulk and confined glassy dynamics, and which clarify the physical connections between these situations, is a high priority. Ideally, theories of interfacial dynamics should be built upon approaches validated in the bulk, and in a manner that minimizes or

eliminates adjustable fit parameters. Moreover, such theories should aim to clarify the importance of the intrinsic space-time dynamic heterogeneity present in bulk liquids⁶³ relative to interfacially induced spatial dynamical heterogeneity (i.e., dynamical gradients) in the thin film dynamics problem.

6. Ongoing theoretical efforts should aim to predict how quantitatively nonuniversal features of glass formation (e.g., fragility) across distinct materials classes (e.g., colloids, molecules, and polymers) and even within a single class (e.g., polymers of diverse monomer structure and backbone stiffness) impact interfacial and thin film effects. This goal is important both for practical materials science and because addressing it will provide additional constraints in the search for a fundamental physical understanding.
7. A concerted effort is needed to better understand short time properties (e.g., Debye-Waller factor and dynamic relaxed plateau shear modulus) under confinement. These quantities carry complementary information about how interfaces strongly modify the microscopic dynamical constraints that underlie the emergence of glassy dynamics and are likely deeply related to the onset question of near-interface dynamic alterations in films and nanostructured materials.
8. New insight is needed into the origin of experimental observations of extremely long range dynamical gradients—100 nm or more in some cases.^{20,207,208} No simulation nor theory of equilibrium gradients has reproduced this finding. These experimental findings, thus far, appear to be limited to polymers at extremely high molecular weights, suggesting that this may be a high-molecular weight polymer effect that will be difficult to access in the simulation, particularly given that the length scales involved also far exceed typical simulation sizes for these systems. A concerted experimental, simulation, and theoretical effort is needed to better understand these findings.

ACKNOWLEDGMENTS

K.S.S. acknowledges support from the U.S. Department of Energy, Office of Science, Basic Energy Sciences, Materials Sciences and Engineering Division, and also from DOE-BES under Grant No. DE-FG02-07ER46471 administered through the Materials Research Laboratory at UIUC.

D.S.S. acknowledges funding from the National Science Foundation under Grant No. CBET1705738.

REFERENCES

- ¹M. Alcoutlabi and G. B. McKenna, *J. Phys.: Condens. Matter* **17**, R461 (2005).
- ²J. Baschnagel and F. Varnik, *J. Phys.: Condens. Matter* **17**, R851 (2005).
- ³C. B. Roth and J. R. Dutcher, *J. Electroanal. Chem.* **584**, 13 (2005).
- ⁴G. B. McKenna, *Eur. Phys. J.: Spec. Top.* **189**, 285 (2010).
- ⁵R. Richert, *Annu. Rev. Phys. Chem.* **62**, 65 (2011).
- ⁶M. D. Ediger and J. A. Forrest, *Macromolecules* **47**, 471 (2014).
- ⁷B. D. Vogt, *J. Polym. Sci., Part B: Polym. Phys.* **56**, 9 (2018).
- ⁸J. A. Forrest, *J. Chem. Phys.* **139**, 084702 (2013).
- ⁹S. Napolitano, E. Glynos, and N. B. Tito, *Rep. Prog. Phys.* **80**, 036602 (2017).
- ¹⁰S. L. Cooper and A. V. Tobolsky, *J. Appl. Polym. Sci.* **10**, 1837 (1966).
- ¹¹J. Bares, *Macromolecules* **8**, 244 (1975).
- ¹²S. Krause, M. Iskandar, and M. Iqbal, *Macromolecules* **15**, 105 (1982).

- ¹³D. Rosati, M. Perrin, P. Navard, V. Harabagiu, M. Pinteala, and B. C. Simionescu, *Macromolecules* **31**, 4301 (1998).
- ¹⁴C. B. Roth and J. M. Torkelson, *Macromolecules* **40**, 3328 (2007).
- ¹⁵C. G. Robertson, T. E. Hogan, M. Rackaitis, J. E. Puskas, and X. Wang, *J. Chem. Phys.* **132**, 104904 (2010).
- ¹⁶M. Z. Slimani, A. J. Moreno, G. Rossi, and J. Colmenero, *Macromolecules* **46**, 5066 (2013).
- ¹⁷D. Christie, R. A. Register, and R. D. Priestley, *ACS Cent. Sci.* **4**, 504 (2018).
- ¹⁸K. Arabeche, L. Delbreilh, J.-M. Saiter, G. H. Michler, R. Adhikari, and E. Baer, *Polymer* **55**, 1546 (2014).
- ¹⁹R. J. Lang, W. L. Merling, and D. S. Simmons, *ACS Macro Lett.* **3**, 758 (2014).
- ²⁰R. R. Baglay and C. B. Roth, *J. Chem. Phys.* **143**, 111101 (2015).
- ²¹C. M. Evans, S. Kim, C. B. Roth, R. D. Priestley, L. J. Broadbelt, and J. M. Torkelson, *Polymer* **80**, 180 (2015).
- ²²S. J. Osborn, M. K. Hassan, G. M. Divoux, D. W. Rhoades, K. A. Mauritz, and R. B. Moore, *Macromolecules* **40**, 3886 (2007).
- ²³R. A. Weiss, *Assignment of the Glass Transition* (ASTM, Philadelphia, PA, 1994), pp. 214–225.
- ²⁴Y. Miwa, T. Kondo, and S. Kutsumizu, *Macromolecules* **46**, 5232 (2013).
- ²⁵D. Ruan and D. S. Simmons, *Macromolecules* **48**, 2313 (2015).
- ²⁶D. Ruan and D. S. Simmons, *J. Polym. Sci., Part B: Polym. Phys.* **53**, 1458 (2015).
- ²⁷Q. Zia, D. Mileva, and R. Androsch, *Macromolecules* **41**, 8095 (2008).
- ²⁸Q. Ma, G. Georgiev, and P. Cebe, *Polymer* **52**, 4562 (2011).
- ²⁹B. Wunderlich, *Prog. Polym. Sci.* **28**, 383 (2003).
- ³⁰C. Schick, A. Wurm, and A. Mohammed, *Thermochim. Acta* **396**, 119 (2003).
- ³¹J. Lin, S. Shenogin, and S. Nazarenko, *Polymer* **43**, 4733 (2002).
- ³²S. M. Aharoni, *Polym. Adv. Technol.* **9**, 169 (1998).
- ³³S. Iannace and L. Nicolais, *J. Appl. Polym. Sci.* **64**, 911 (1997).
- ³⁴J. Lee, J. H. Mangalana, and D. S. Simmons, *J. Polym. Sci., Part B: Polym. Phys.* **55**, 907 (2017).
- ³⁵F. W. Starr and J. F. Douglas, *Phys. Rev. Lett.* **106**, 115702 (2011).
- ³⁶B. A. P. Betancourt, J. F. Douglas, and F. W. Starr, *Soft Matter* **9**, 241 (2012).
- ³⁷F. W. Starr, T. B. Schröder, and S. C. Glotzer, *Phys. Rev. E* **64**, 021802 (2001).
- ³⁸A. Bansal, H. Yang, C. Li, K. Cho, B. C. Benicewicz, S. K. Kumar, and L. S. Schadler, *Nat. Mater.* **4**, 693 (2005).
- ³⁹J. Jancar, J. F. Douglas, F. W. Starr, S. K. Kumar, P. Cassagnau, A. J. Lesser, S. Sternstein, and M. J. Buehler, *Polymer* **51**, 3321 (2010).
- ⁴⁰G. D. Hattener and G. Arya, *Macromolecules* **48**, 1240 (2015).
- ⁴¹Y. Termonia, *J. Polym. Sci., Part B: Polym. Phys.* **48**, 687 (2010).
- ⁴²A. Papon, H. Montes, M. Hanafi, F. Lequeux, L. Guy, and K. Saalwächter, *Phys. Rev. Lett.* **108**, 065702 (2012).
- ⁴³Y. Guo, C. Zhang, C. Lai, R. D. Priestley, M. D'Acunzi, and G. Fytas, *ACS Nano* **5**, 5365 (2011).
- ⁴⁴C. Zhang, Y. Guo, and R. D. Priestley, *Macromolecules* **44**, 4001 (2011).
- ⁴⁵W. L. Merling, J. B. Mileski, J. F. Douglas, and D. S. Simmons, *Macromolecules* **49**, 7597 (2016).
- ⁴⁶S. Sahoo and A. K. Bhowmick, *J. Appl. Polym. Sci.* **106**, 3077 (2007).
- ⁴⁷J. Berriot, H. Montes, F. Lequeux, D. Long, and P. Sotta, *Europhys. Lett.* **64**, 50 (2003).
- ⁴⁸J. Berriot, H. Montes, F. Lequeux, D. Long, and P. Sotta, *Macromolecules* **35**, 9756 (2002).
- ⁴⁹A. Papon, K. Saalwächter, K. Schäler, L. Guy, F. Lequeux, and H. Montes, *Macromolecules* **44**, 913 (2011).
- ⁵⁰C. L. Jackson and G. B. McKenna, *J. Non-Cryst. Solids* **131–133**, 221 (1991).
- ⁵¹C. L. Jackson and G. B. McKenna, *Chem. Mater.* **8**, 2128 (1996).
- ⁵²W. Humprey, A. Dalke, and K. Schulten, *J. Mol. Graphics* **14**, 33 (1996).
- ⁵³S. P. Delcambre, R. A. Riggelman, J. J. de Pablo, and P. F. Nealey, *Soft Matter* **6**, 2475 (2010).
- ⁵⁴W.-F. Kuan, R. Remy, M. E. Mackay, and T. H. Epps III, *RSC Adv.* **5**, 12597 (2015).
- ⁵⁵V. Sethuraman and V. Ganesan, *Soft Matter* **12**, 7818 (2016).
- ⁵⁶J. H. Mangalana, M. D. Marvin, and D. S. Simmons, *J. Phys. Chem. B* **120**, 4861 (2016).
- ⁵⁷M. D. Ediger, J. de Pablo, and L. Yu, *Acc. Chem. Res.* **52**, 407 (2019).
- ⁵⁸M. D. Ediger, *J. Chem. Phys.* **147**, 210901 (2017).
- ⁵⁹L. Zhu, C. W. Brian, S. F. Swallen, P. T. Straus, M. D. Ediger, and L. Yu, *Phys. Rev. Lett.* **106**, 256103 (2011).
- ⁶⁰W. Zhang and L. Yu, *Macromolecules* **49**, 731 (2016).
- ⁶¹Z. Fakhraai and J. A. Forrest, *Phys. Rev. Lett.* **95**, 025701 (2005).
- ⁶²J. A. Forrest and K. Dalnoki-Veress, *Adv. Colloid Interface Sci.* **94**, 167 (2001).
- ⁶³L. Berthier and G. Biroli, *Rev. Mod. Phys.* **83**, 587 (2011).
- ⁶⁴C. Cammarota and G. Biroli, *J. Chem. Phys.* **138**, 12A547 (2013).
- ⁶⁵R. Richert, in *Structural Glasses and Supercooled Liquids*, edited by P. G. Wolynes and V. Lubchenko (John Wiley & Sons, Inc., 2012), pp. 1–30.
- ⁶⁶D. Cangialosi, V. M. Boucher, A. Alegria, and J. Colmenero, *Soft Matter* **9**, 8619 (2013).
- ⁶⁷J.-H. Hung, T. K. Patra, V. Meenakshisundaram, J. H. Mangalana, and D. S. Simmons, *Soft Matter* **15**, 1223 (2018).
- ⁶⁸S. Peter, H. Meyer, and J. Baschnagel, *J. Polym. Sci., Part B: Polym. Phys.* **44**, 2951 (2006).
- ⁶⁹P. Scheidler, W. Kob, and K. Binder, *Europhys. Lett.* **59**, 701 (2002).
- ⁷⁰F. Varnik, J. Baschnagel, and K. Binder, *Phys. Rev. E* **65**, 021507 (2002).
- ⁷¹P. Scheidler, W. Kob, and K. Binder, *Eur. Phys. J. E* **12**, 5 (2003).
- ⁷²P. Scheidler, W. Kob, and K. Binder, *J. Phys. Chem. B* **108**, 6673 (2004).
- ⁷³D. Diaz-Vela, J.-H. Hung, and D. S. Simmons, *ACS Macro Lett.* **7**, 1295 (2018).
- ⁷⁴W. Kob, S. Roldán-Vargas, and L. Berthier, *Nat. Phys.* **8**, 164 (2012).
- ⁷⁵D. S. Simmons, *Macromol. Chem. Phys.* **217**, 137 (2016).
- ⁷⁶S. A. Kivelson and G. Tarjus, *Nat. Mater.* **7**, 831 (2008).
- ⁷⁷A. Cavagna, *Phys. Rep.* **476**, 51 (2009).
- ⁷⁸J. H. Mangalana, M. E. Mackura, M. D. Marvin, and D. S. Simmons, *J. Chem. Phys.* **146**, 203316 (2017).
- ⁷⁹C. Ye, C. G. Weiner, M. Tyagi, D. Uhrig, S. V. Orski, C. L. Soles, B. D. Vogt, and D. S. Simmons, *Macromolecules* **48**, 801 (2015).
- ⁸⁰J. E. Pye, K. A. Rohald, E. A. Baker, and C. B. Roth, *Macromolecules* **43**, 8296 (2010).
- ⁸¹M. D. Marvin, R. J. Lang, and D. S. Simmons, *Soft Matter* **10**, 3166 (2014).
- ⁸²R. J. Lang and D. S. Simmons, *Macromolecules* **46**, 9818 (2013).
- ⁸³J. A. Forrest and K. Dalnoki-Veress, *ACS Macro Lett.* **3**, 310 (2014).
- ⁸⁴S. Kim, S. A. Hewlett, C. B. Roth, and J. M. Torkelson, *Eur. Phys. J. E* **30**, 83 (2009).
- ⁸⁵S. Mirigian and K. S. Schweizer, *J. Chem. Phys.* **141**, 161103 (2014).
- ⁸⁶J. E. G. Lipson and S. T. Milner, *Eur. Phys. J. B* **72**, 133 (2009).
- ⁸⁷C. Rotella, M. Wübbenhorst, and S. Napolitano, *Soft Matter* **7**, 5260 (2011).
- ⁸⁸S. Mirigian and K. S. Schweizer, *J. Chem. Phys.* **143**, 244705 (2015).
- ⁸⁹J. E. G. Lipson and S. T. Milner, *Macromolecules* **43**, 9874 (2010).
- ⁹⁰W. Zhang, J. F. Douglas, and F. W. Starr, *Proc. Natl. Acad. Sci. U. S. A.* **115**, 5641–5646 (2018).
- ⁹¹Z. Fakhraai and J. A. Forrest, *Science* **319**, 600 (2008).
- ⁹²C. R. Daley, Z. Fakhraai, M. D. Ediger, and J. A. Forrest, *Soft Matter* **8**, 2206 (2012).
- ⁹³E. C. Glor, R. J. Composto, and Z. Fakhraai, *Macromolecules* **48**, 6682 (2015).
- ⁹⁴Y. Zhang, E. C. Glor, M. Li, T. Liu, K. Wahid, W. Zhang, R. A. Riggelman, and Z. Fakhraai, *J. Chem. Phys.* **145**, 114502 (2016).
- ⁹⁵Y. Zhang, C. N. Woods, M. Alvarez, Y. Jin, R. A. Riggelman, and Z. Fakhraai, *J. Chem. Phys.* **149**, 184902 (2018).
- ⁹⁶S. Mirigian and K. S. Schweizer, *J. Chem. Phys.* **140**, 194506 (2014).
- ⁹⁷F. W. Starr, J. F. Douglas, and S. Sastry, *J. Chem. Phys.* **138**, 12A541 (2013).
- ⁹⁸M. D. Ediger and P. Harrowell, *J. Chem. Phys.* **137**, 080901 (2012).
- ⁹⁹T. B. Schröder, S. Sastry, J. C. Dyre, and S. C. Glotzer, *J. Chem. Phys.* **112**, 9834–9840 (2000).
- ¹⁰⁰J. Dudowicz, K. F. Freed, and J. F. Douglas, *Advances in Chemical Physics* (Wiley, 2008), pp. 125–222.
- ¹⁰¹S. Napolitano and M. Wübbenhorst, *Polymer* **51**, 5309 (2010).

- ¹⁰²G. M. Hocky, L. Berthier, W. Kob, and D. R. Reichman, *Phys. Rev. E* **89**, 052311 (2014).
- ¹⁰³Y. Zhou and S. T. Milner, *Macromolecules* **50**, 5599 (2017).
- ¹⁰⁴C. J. Ellison and J. M. Torkelson, *Nat. Mater.* **2**, 695 (2003).
- ¹⁰⁵R. D. Priestley, C. J. Ellison, L. J. Broadbelt, and J. M. Torkelson, *Science* **309**, 456 (2005).
- ¹⁰⁶K. Paeng and M. D. Ediger, *Macromolecules* **44**, 7034 (2011).
- ¹⁰⁷K. Paeng, R. Richert, and M. D. Ediger, *Soft Matter* **8**, 819 (2011).
- ¹⁰⁸K. Paeng, S. F. Swallen, and M. D. Ediger, *J. Am. Chem. Soc.* **133**, 8444 (2011).
- ¹⁰⁹J. H. Teichroeb and J. A. Forrest, *Phys. Rev. Lett.* **91**, 016104 (2003).
- ¹¹⁰M. Ilton, D. Qi, and J. A. Forrest, *Macromolecules* **42**, 6851 (2009).
- ¹¹¹S. A. Hutcheson and G. B. McKenna, *Phys. Rev. Lett.* **94**, 076103 (2005).
- ¹¹²Y. Chai, T. Salez, J. D. McGraw, M. Benzaquen, K. Dalnoki-Veress, E. Raphael, and J. A. Forrest, *Science* **343**, 994 (2014).
- ¹¹³M. Chowdhury, Y. Guo, Y. Wang, W. L. Merling, J. H. Mangalala, D. S. Simmons, and R. D. Priestley, *J. Phys. Chem. Lett.* **8**, 1229 (2017).
- ¹¹⁴A. Shavit and R. A. Riggleman, *Macromolecules* **46**, 5044 (2013).
- ¹¹⁵T. S. Jain and J. J. de Pablo, *Phys. Rev. Lett.* **92**, 155505 (2004).
- ¹¹⁶H. Morita, K. Tanaka, T. Kajiyama, T. Nishi, and M. Doi, *Macromolecules* **39**, 6233 (2006).
- ¹¹⁷R. A. Riggleman, K. Yoshimoto, J. F. Douglas, and J. J. de Pablo, *Phys. Rev. Lett.* **97**, 045502 (2006).
- ¹¹⁸S. Peter, H. Meyer, J. Baschnagel, and R. Seemann, *J. Phys.: Condens. Matter* **19**, 205119 (2007).
- ¹¹⁹A. Shavit and R. A. Riggleman, *J. Phys. Chem. B* **118**, 9096 (2014).
- ¹²⁰J. H. Mangalala, M. D. Marvin, N. R. Wiener, M. E. Mackura, and D. S. Simmons, *J. Chem. Phys.* **146**, 104902 (2017).
- ¹²¹D. D. Hsu, W. Xia, J. Song, and S. Ketten, *ACS Macro Lett.* **5**, 481 (2016).
- ¹²²J. A. Torres, P. F. Nealey, and J. J. de Pablo, *Phys. Rev. Lett.* **85**, 3221 (2000).
- ¹²³P. Z. Hanakata, J. F. Douglas, and F. W. Starr, *J. Chem. Phys.* **137**, 244901 (2012).
- ¹²⁴P. Z. Hanakata, J. F. Douglas, and F. W. Starr, *Nat. Commun.* **5**, 4163 (2014).
- ¹²⁵W. Zhang, J. F. Douglas, and F. W. Starr, *J. Chem. Phys.* **147**, 044901 (2017).
- ¹²⁶M. Z. Slimani, A. J. Moreno, and J. Colmenero, *Macromolecules* **44**, 6952 (2011).
- ¹²⁷M. Z. Slimani, A. J. Moreno, and J. Colmenero, *Macromolecules* **45**, 8841 (2012).
- ¹²⁸J.-Y. Park and G. B. McKenna, *Phys. Rev. B* **61**, 6667 (2000).
- ¹²⁹W. Kob and D. Coslovich, *Phys. Rev. E* **90**, 052305 (2014).
- ¹³⁰M. Tress, M. Erber, E. U. Mapesa, H. Huth, J. Müller, A. Sergei, C. Schick, K.-J. Eichhorn, B. Voit, and F. Kremer, *Macromolecules* **43**, 9937 (2010).
- ¹³¹J. S. Sharp and J. A. Forrest, *Phys. Rev. E* **67**, 031805 (2003).
- ¹³²V. M. Boucher, D. Cangialosi, H. Yin, A. Schönhals, A. Alegria, and J. Colmenero, *Soft Matter* **8**, 5119 (2012).
- ¹³³Z. Yang, Y. Fujii, F. K. Lee, C.-H. Lam, and O. K. C. Tsui, *Science* **328**, 1676 (2010).
- ¹³⁴S. F. Swallen, P. A. Bonvallet, R. J. McMahon, and M. D. Ediger, *Phys. Rev. Lett.* **90**, 015901 (2003).
- ¹³⁵M. K. Mapesa, S. F. Swallen, and M. D. Ediger, *J. Phys. Chem. B* **110**, 507 (2006).
- ¹³⁶J.-H. Hung, J. H. Mangalala, and D. S. Simmons, *Macromolecules* **51**, 2887 (2018).
- ¹³⁷B. Schmidtke, N. Petzold, R. Kahlau, M. Hofmann, and E. A. Rössler, *Phys. Rev. E* **86**, 041507 (2012).
- ¹³⁸N. Petzold, B. Schmidtke, R. Kahlau, D. Bock, R. Meier, B. Micko, D. Kruk, and E. A. Rössler, *J. Chem. Phys.* **138**, 12A510 (2013).
- ¹³⁹B. Schmidtke, M. Hofmann, A. Lichtinger, and E. A. Rössler, *Macromolecules* **48**, 3005 (2015).
- ¹⁴⁰E. C. Glor and Z. Fakhraai, *J. Chem. Phys.* **141**, 194505 (2014).
- ¹⁴¹H. Vogel, *Phys. Z.* **22**, 645 (1921).
- ¹⁴²G. S. Fulcher, *J. Am. Ceram. Soc.* **8**, 339 (1925).
- ¹⁴³G. Tammann and W. Hesse, *Z. Anorg. Allg. Chem.* **156**, 245 (1926).
- ¹⁴⁴L. Berthier and W. Kob, *Phys. Rev. E* **85**, 011102 (2012).
- ¹⁴⁵Y.-W. Li, Y.-L. Zhu, and Z.-Y. Sun, *J. Chem. Phys.* **142**, 124507 (2015).
- ¹⁴⁶D. M. Sussman, S. S. Schoenholz, E. D. Cubuk, and A. J. Liu, *Proc. Natl. Acad. Sci. U. S. A.* **114**, 10601 (2017).
- ¹⁴⁷S. S. Schoenholz, E. D. Cubuk, D. M. Sussman, E. Kaxiras, and A. J. Liu, *Nat. Phys.* **12**, 469 (2016).
- ¹⁴⁸F. He, L. M. Wang, and R. Richert, *Phys. Rev. B* **71**, 144205 (2005).
- ¹⁴⁹P. Z. Hanakata, B. A. P. Betancourt, J. F. Douglas, and F. W. Starr, *J. Chem. Phys.* **142**, 234907 (2015).
- ¹⁵⁰D. S. Fryer, R. D. Peters, E. J. Kim, J. E. Tomaszewski, P. F. Nealey, C. C. White, and W. L. Wu, *Macromolecules* **34**, 5627 (2001).
- ¹⁵¹J. H. van Zanten and K. P. Rufefer, *Phys. Rev. E* **62**, 5389 (2000).
- ¹⁵²J. Yang and K. S. Schweizer, *J. Chem. Phys.* **134**, 204909 (2011).
- ¹⁵³M. T. Cicerone and C. L. Soles, *Biophys. J.* **86**, 3836 (2004).
- ¹⁵⁴D. S. Simmons and J. F. Douglas, *Soft Matter* **7**, 11010 (2011).
- ¹⁵⁵S. Cheng, S. Mirigian, J.-M. Y. Carrillo, V. Bocharova, B. G. Sumpter, K. S. Schweizer, and A. P. Sokolov, *J. Chem. Phys.* **143**, 194704 (2015).
- ¹⁵⁶B. Carroll, S. Cheng, and A. P. Sokolov, *Macromolecules* **50**, 6149 (2017).
- ¹⁵⁷S. Cheng, B. Carroll, V. Bocharova, J.-M. Carrillo, B. G. Sumpter, and A. P. Sokolov, *J. Chem. Phys.* **146**, 203201 (2017).
- ¹⁵⁸J. Berriot, F. Lequeux, L. Monnerie, H. Montes, D. Long, and P. Sotta, *J. Non-Cryst. Solids* **307-310**, 719 (2002).
- ¹⁵⁹S. Y. Kim, H. W. Meyer, K. Saalwächter, and C. F. Zukoski, *Macromolecules* **45**, 4225 (2012).
- ¹⁶⁰P. A. O'Connell, S. A. Hutcheson, and G. B. McKenna, *J. Polym. Sci., Part B: Polym. Phys.* **46**, 1952 (2008).
- ¹⁶¹P. A. O'Connell, J. Wang, T. A. Ishola, and G. B. McKenna, *Macromolecules* **45**, 2453 (2012).
- ¹⁶²E. C. Glor, G. V. Angrand, and Z. Fakhraai, *J. Chem. Phys.* **146**, 203330 (2017).
- ¹⁶³J. E. Pye and C. B. Roth, *Phys. Rev. Lett.* **107**, 235701 (2011).
- ¹⁶⁴W. Kauzmann, *Chem. Rev.* **43**, 219 (1948).
- ¹⁶⁵G. Adam and J. H. Gibbs, *J. Chem. Phys.* **43**, 139 (1965).
- ¹⁶⁶T. R. Kirkpatrick and D. Thirumalai, in *Structural Glasses and Supercooled Liquids*, edited by P. G. Wolynes and V. Lubchenko (John Wiley & Sons, Inc., 2012), pp. 223–236.
- ¹⁶⁷V. Lubchenko and P. G. Wolynes, *Annu. Rev. Phys. Chem.* **58**, 235 (2007).
- ¹⁶⁸B. A. P. Betancourt, J. F. Douglas, and F. W. Starr, *J. Chem. Phys.* **140**, 204509 (2014).
- ¹⁶⁹T. M. Truskett and V. Ganesan, *J. Chem. Phys.* **119**, 1897 (2003).
- ¹⁷⁰K. Fukao and Y. Miyamoto, *Phys. Rev. E* **64**, 011803 (2001).
- ¹⁷¹M. Ozawa, C. Scalliet, A. Ninarello, and L. Berthier, e-print [arXiv:1905.08179](https://arxiv.org/abs/1905.08179) [Cond-Mat] (2019).
- ¹⁷²J. D. Stevenson and P. G. Wolynes, *J. Chem. Phys.* **129**, 234514 (2008).
- ¹⁷³W. Götze, *Complex Dynamics of Glass-Forming Liquids: A Mode-Coupling Theory* (Oxford University Press, 2008).
- ¹⁷⁴W. Zhang, F. W. Starr, and J. F. Douglas, *J. Phys. Chem. B* **123**, 5935–5941 (2019).
- ¹⁷⁵R. P. White and J. E. Lipson, *Macromolecules* **49**, 3987 (2016).
- ¹⁷⁶J. D. McCoy and J. G. Curro, *J. Chem. Phys.* **116**, 9154 (2002).
- ¹⁷⁷G. S. Grest and M. H. Cohen, *Advances in Chemical Physics* (John Wiley & Sons, Ltd., 2007), pp. 455–525.
- ¹⁷⁸D. Long and F. Lequeux, *Eur. Phys. J. E* **4**, 371 (2001).
- ¹⁷⁹S. Merabia, P. Sotta, and D. Long, *Eur. Phys. J. E* **15**, 189 (2004).
- ¹⁸⁰T. Salez, J. Salez, K. Dalnoki-Veress, E. Raphaël, and J. A. Forrest, *Proc. Natl. Acad. Sci. U. S. A.* **112**, 8227 (2015).
- ¹⁸¹R. P. White and J. E. G. Lipson, *J. Chem. Phys.* **147**, 184503 (2017).
- ¹⁸²R. P. White and J. E. G. Lipson, *Eur. Phys. J. E* **42**, 100 (2019).
- ¹⁸³R. P. White, J. E. G. Lipson, and J. S. Higgins, *Macromolecules* **45**, 8861 (2012).
- ¹⁸⁴R. P. White, J. E. G. Lipson, and J. S. Higgins, *Macromolecules* **45**, 1076 (2012).
- ¹⁸⁵R. P. White and J. E. G. Lipson, *ACS Macro Lett.* **4**, 588 (2015).
- ¹⁸⁶R. Casalini, U. Mohanty, and C. M. Roland, *J. Chem. Phys.* **125**, 014505 (2006).
- ¹⁸⁷D. Coslovich and C. M. Roland, *J. Phys. Chem. B* **112**, 1329 (2008).
- ¹⁸⁸R. P. White and J. E. G. Lipson, *Macromolecules* **51**, 7924 (2018).

- ¹⁸⁹A. Debot, R. P. White, J. E. G. Lipson, and S. Napolitano, *ACS Macro Lett.* **8**, 41 (2019).
- ¹⁹⁰D. Chandler and J. P. Garrahan, *Annu. Rev. Phys. Chem.* **61**, 191 (2010).
- ¹⁹¹N. B. Tito, J. E. G. Lipson, and S. T. Milner, *Soft Matter* **9**, 3173 (2013).
- ¹⁹²N. B. Tito, J. E. G. Lipson, and S. T. Milner, *Soft Matter* **9**, 9403 (2013).
- ¹⁹³J. DeFelice and J. E. G. Lipson, *Soft Matter* **15**, 1651 (2019).
- ¹⁹⁴J. C. Dyre, *Rev. Mod. Phys.* **78**, 953 (2006).
- ¹⁹⁵J. C. Dyre, *J. Non-Cryst. Solids* **235**, 142 (1998).
- ¹⁹⁶J. C. Dyre, T. Christensen, and N. B. Olsen, *J. Non-Cryst. Solids* **352**, 4635 (2006).
- ¹⁹⁷S. Mirigian and K. S. Schweizer, *J. Chem. Phys.* **140**, 194507 (2014).
- ¹⁹⁸K. S. Schweizer, *J. Chem. Phys.* **123**, 244501 (2005).
- ¹⁹⁹E. J. Saltzman and K. S. Schweizer, *Phys. Rev. E* **77**, 051504 (2008).
- ²⁰⁰S. Mirigian and K. S. Schweizer, *Macromolecules* **48**, 1901 (2015).
- ²⁰¹S. J. Xie and K. S. Schweizer, *Macromolecules* **49**, 9655 (2016).
- ²⁰²S. Mirigian and K. S. Schweizer, *J. Chem. Phys.* **146**, 203301 (2017).
- ²⁰³A. D. Phan and K. S. Schweizer, *Macromolecules* **51**, 6063 (2018).
- ²⁰⁴A. D. Phan and K. S. Schweizer, *J. Chem. Phys.* **150**, 044508 (2019).
- ²⁰⁵A. D. Phan and K. S. Schweizer, *Macromolecules* **52**, 5192 (2019).
- ²⁰⁶A. D. Phan and K. S. Schweizer, "Influence of the longer range spatial transfer of solid surface induced change of caging constraints on the heterogeneous dynamics of glass-forming liquids," *ACS Macro Lett.* (unpublished).
- ²⁰⁷R. R. Baglay and C. B. Roth, *J. Chem. Phys.* **146**, 203307 (2017).
- ²⁰⁸T. Lan and J. M. Torkelson, *Macromolecules* **49**, 1331 (2016).